FINAL TECHNICAL REPORT

PALEOSEISMIC INVESTIGATIONS OF HOLOCENE EARTHQUAKE RECURRENCE ON THE PENINSULA SEGMENT OF THE SAN ANDREAS FAULT, WOODSIDE, CA:

JOINT PROJECT BETWEEN
FUGRO CONSULTANTS INC.,AECOM, AND THE UNITED STATES GEOLOGICAL SURVEY

Prepared for
U.S. Geological Survey
National Earthquake Hazards Reduction Program
Award Numbers G12AP20060 and G12AP20061

July 2015

FINAL TECHNICAL REPORT

PALEOSEISMIC INVESTIGATIONS OF HOLOCENE EARTHQUAKE RECURRENCE ON THE PENINSULA SEGMENT OF THE SAN ANDREAS FAULT, WOODSIDE, CA: JOINT PROJECT BETWEEN FUGRO CONSULTANTS INC., AECOM, AND THE UNITED STATES GEOLOGICAL SURVEY

Principal Investigators:
Özgür Kozacı, Fugro Consultants Inc.
(Award G12AP20060)
1777 Botelho Dr., Suite 262, Walnut Creek, CA 945961
(925)256-6070 (phone); (925)256-6076 (fax)
o.kozaci@fugro.com

Judith Zachariasen, AECOM
(Award G12AP20061)
1333 Broadway, Suite 800, Oakland, CA 94612
(510) 874-1749 (phone); (510) 874-3268 (fax);
judy.zachariasen@aecom.com

Carol Prentice, U.S. Geological Survey
345 Middlefield Road, M.S. 977, Menlo Park, CA 94025
650-329-5690 (phone); 650-329-5163 (fax)
cprentice@usgs.gov

Program Elements I and III
Northern California Region

Keywords:
Quaternary fault behavior, neotectonics, paleoseismology

U. S. Geological Survey
National Earthquake Hazards Reduction Program

July 2015

This research was supported by the U.S. Geological Survey (USGS), Department of the Interior, under USGS Awards G12AP20060 and G12AP20061. The views and conclusions contained in this document are those of the Principal Investigators only and should not be interpreted as necessarily representing the official policies, either expressed or implied, of the U.S. Government.

ABSTRACT

The San Andreas fault (SAF) through the San Francisco peninsula region poses a significant hazard to the San Francisco Bay area, but the earthquake history of the Peninsula section of the SAF (SAP) remains enigmatic. Little is known about the timing of earthquakes on this section of the fault prior to the great earthquake of April 18, 1906. An earthquake in 1838, with an estimated magnitude between M6.8 and 7.4, produced strong shaking on the San Francisco Peninsula, and many people have assumed that this event occurred on the SAF. However, paleoseismic excavations across the fault at several sites on the Peninsula have failed to provide affirmative evidence that the 1838 earthquake was associated with surface rupture on the SAF. The lack of a robust paleoseismic history means that the seismic hazard posed by the northern SAF to the San Francisco Bay Area is poorly understood - does the fault rupture only in large 1906-style events, or also in smaller, localized events, perhaps limited to the Peninsula or smaller sections? In this study, we have aimed to address the lack of a well-constrained earthquake history by acquiring paleoseismic and displacement data from trenches at the Crystal Springs South (CSS) site on the Peninsula section of the SAP, near Woodside, CA.

This study further develops the CSS trench site whose earlier results were presented in Zachariasen et al., 2011) and related abstracts (e.g. Zachariasen et al., 2010; Prentice et al., 2011; 2012). The site is located about 1.2 km southeast of Crystal Springs Reservoir. In the first phase of investigation, we excavated two trenches across the fault and exposed fluvial gravel and floodbank deposits overlying an older weathered, clay-rich colluvial unit. The fluvial deposits have been cut by two distinct generations of faults. The younger set of faults breaks nearly to the ground surface, and we interpret these faults to represent surface faulting during the 1906 San Francisco earthquake that has been buried by post-1906 sediments. The older faults terminate below a colluvial wedge derived from one of the fluvial gravel deposits. The older event, marked by the presence of a colluvial wedge between dated overbank deposits, occurred about AD 1000 (994-1018 cal AD). We found no evidence of the 1838 earthquake.

For this project, we excavated another fault perpendicular trench that confirmed the previous event stratigraphy. In addition, we excavated three fault parallel trenches between the fault perpendicular trenches. These trenches exposed a buried fluvial channel offset 6-8 m by the SAF. The 6-8 m offset of the channel deposit is consistent with offset in only two 1906-size events and inconsistent with more than three 1906-size events. This suggests that whereas one event could be missing from the section exposed at the CSS site, it is unlikely that many large events have gone unrecognized. More frequent smaller-offset events may have accommodated the observed offset, but they are not preserved as distinct event horizons in the stratigraphic record. The late Holocene slip rate for this part of the fault has been calculated to be 17±4 mm/yr. The fact that only 6-8 m of slip has accumulated at this site in the last ~1000 years indicates a slip deficit on the fault here, suggesting that either the slip rate is variable on millennial timescales or that significant slip is accommodated off the faults exposed during this study.

In previous studies at Portola Valley to the southeast, evidence of three, possibly four, events in ~1000 years was observed. At the new Scarp Creek paleoseismic site at Filoli Estates, about 0.5 km south of the CSS site, results indicate at least three events have occurred in about 900 years (Prentice et al., 2014). At these other sites, as at the CSS site, there is no affirmative evidence of the postulated 1838 earthquake, although it is permissible at Portola Valley and the new Filoli site. The hundreds-of-years interval between the 1906 and prior events at the CSS site and other sites on the Peninsula, contrasts with the records at sites along the Santa Cruz Mountains segments, which have much shorter intervals between events. This disparity calls into question preferred seismic hazard models in which the entire northern San Andreas fault ruptures together, similar to the 1906 rupture. It may be as or more common that different parts of the fault rupture independently, yielding different rupture histories at different locations along the fault.

TABLE OF CONTENTS

Final Technical Report 1
1.0 Introduction 5
2.0 Previous Work 7
2.1 1906 Earthquake 7
2.2 Paleoseismic Studies 7
3.0 Crystal Springs South (CSS) Site 9
3.1 Setting 9
3.2 Methods 9
3.3 Trench Stratigraphy 10
3.3.1 Cross-fault Trenches 10
Trench T2 10
Trench T1 11
Trench T6 12
3.3.2 Fault-parallel trenches 13
Trench T3 13
Trench T4 13
Trench T5 and T5b 14
3.4 Age Constraints 14
3.5 Fault Displacement 15
4.0 Discussion 16
5.0 Conclusions 18
6.0 Acknowledgments 19
7.0 References 20
Appendix 23

LIST OF TABLES AND FIGURES

Table 1. Radiocarbon ages of samples from Crystal Springs South Site trenches

Figure 1. Map of the northern San Andreas fault system, including the Peninsula segment (SAP). From WGCEP (2003).

Figure 2. San Andreas fault Peninsula segment near Woodside, CA.

Figure 3. Aerial Photograph of Crystal Springs South site

Figure 4. Site map. Bare earth DEM obtained from LiDAR data of Crystal Springs South site.

Figure 5. Map of trench site locations.

Figure 6. Photograph of trenches T1 and T2.

Figure 7a. Log of southeast wall of trench T2.

Figure 7b. Log of northwest wall of trench T2.

Figure 8. Log of northwest wall of trench T1.

Figure 9. Photograph of trenches T5 and T6.

Figure 10. Log of trench T3.

Figure 11. Log of trench T4.

Figure 12. Log of trench T5.

Figure 13. Log of trench T6.

Figure 14. Close-up of the fault zone in the southern wall of Trench T2 with radiocarbon samples.

Figure 15. OxCal model showing age constraints on "Event G" and on offset channel.

Figure 16. Map showing all trench locations and offset buried channel

1.0 INTRODUCTION

The northern SAF last ruptured in the 1906 **M** 7.9 San Francisco earthquake along its full extent from the northern end of the creeping segment near San Juan Bautista to Shelter Cove near the Mendocino triple junction (Figure 1). The Working Groups on California Earthquake Probabilities (2003, 2008, hereinafter referred to as WGCEP, 2003, 2008), building on models of previous working groups (e.g. WGCEP, 1988, 1990; WGNCEP, 1996), divided the northern SAF into four segments, which differ from one another in one or more characteristics, such as average strike, slip rate, recurrence interval, and age of penultimate earthquake. These segments, from north to south, include Offshore (SAO), North Coast (SAN), Peninsula (SAP), and Santa Cruz Mountains (SAS) (Figure 1). These segments are assumed to rupture in characteristic ways, with earthquakes constrained to single segments or combinations of entire segments, such as the multi-segment rupture of the northern SAF as in 1906. The most recent statewide hazard assessment, UCERF3 (Field et al., 2013), relaxes the strict segmentation model of faults, recognizing that successive ruptures on a fault or fault system may not always be defined by exactly the same segment boundaries. They divide faults into small sections and permit greater flexibility in the combined rupture of adjacent sections.

The Peninsula segment as defined by the WGCEP (2003) is about 85 km long and extends from the Golden Gate southward to the north end of the Loma Prieta aftershock zone (WGNCEP, 1996; 2003; Figure 1). It is flanked to the north by the North Coast segment and to the south by the Santa Cruz Mountains segment. The northern end of the Peninsula segment coincides with the junction of the San Gregorio fault and the San Andreas fault. Average slip in the 1906 earthquake decreased south of the Golden Gate from about 5 m to about 3 m. The southern end of the segment coincides with a restraining bend in the fault and a lithologic change.

The working groups developed assessments of earthquake probability on the San Andreas fault based on interpretations of the data and expert opinion regarding the mode of failure of paleo- and ostensibly future earthquakes. These assessments are highly dependent on estimates of the likelihood that long multi-section ruptures are more or less common than shorter ruptures. Such estimates are themselves dependent on the rupture behavior of past earthquakes and thus on the paleoseismic record of different sections and indeed along the length of the fault. To date, the paleo-earthquake record on the northern San Andreas is incomplete, with few paleoseismic sites recording more than a small number of events. Thus, a key element to improving the assessment of northern San Andreas earthquake probabilities is to improve the paleoseismic record so as to test different rupture models. This study addresses this issue by providing further paleoseismic data on the SAP, a section of the SAF that currently has a limited record of paleoearthquakes.

The working groups prefer rupture models that involve failure of the entire northern San Andreas fault, as in 1906, based on similar ages for some events observed at paleoseismic sites on the SAS and SAN segments, which have been inferred to be the same event. However, the timing of some past events at paleoseismic sites on the SAS differs from that on other sections, suggesting that at least some earthquakes involve smaller ruptures. The working groups have favored rupture models in which the smaller events involve rupture of SAS and SAP together rather than independently. The result of the working group assessments is that seismic hazard from the northern San Andreas fault is dominated by larger, more infrequent events. This result is strongly dependent on assumptions about behavior of the Peninsula segment that is poorly constrained by paleoseismic data. There is no site on the Peninsula segment to date with a well-developed event chronology. If the Peninsula were shown to have a very different recurrence from sections to the north and south, smaller ruptures would become commensurately more significant in the fault model and the hazard could be different, with a greater contribution from

smaller but more frequent earthquakes. In order to assess the validity of the seismic hazard model, it is crucial that a robust paleoearthquake record be developed on the peninsula.

The age and extent of the penultimate event on the Peninsula segment is unknown, and constraints on older events are minimal to nonexistent. Modeling of intensity data by Toppozada and Borchardt (1998) and Bakun (1999) indicates that the 1838 historical earthquake, which has magnitude estimates of **M** 6.8-7.4, was located on the peninsula. The San Andreas fault has been proposed as the likely fault, but direct evidence for the event on the SAP is lacking. Hall et al. (1999) interpreted offsets of stream channels at the Filoli paleoseismic site (Figure 2) to indicate a pre-1906 earthquake that occurred after deposition of deposits dated to AD 1420-1820. The inferred slip in that event was about 60% of that in 1906, leading them to conclude that the penultimate event ruptured a shorter length of the fault, possibly only the Peninsula segment. They tentatively equate this paleoearthquake with the 1838 earthquake, but, whereas it is a plausible explanation, there is no direct evidence that the two events are one and the same. Paleoseismic work on the Peninsula segment at the Crystal Springs and Portola Valley sites (Figure 2) revealed no evidence for the 1838 earthquake (Baldwin et al., 2006; Prentice and Moreno, 2007; Prentice et al., 2008; Sundermann et al., 2008). Nevertheless, the postulated interpretations of relatively inconclusive data from Filoli have been part of the basis for rupture modeling of the northern San Andreas fault and consequently for the assessment of seismic hazard posed by the fault to the San Francisco Bay Area.

In an effort to shed further light on the earthquake history of the Peninsula section of the SAF, we have developed another paleoseismic site south of Crystal Springs reservoir and north of Filoli Estates, the Crystal Springs South site. In 2010, we excavated two fault perpendicular trenches and documented evidence for two surface ruptures on the fault within the last ca. 900 years (Prentice et al, 2011; Zachariasen et al., 2011).

In this report, we present the results of additional trenching studies at the CSS site from 2011 and 2012. We excavated an additional fault-perpendicular trench, along with three fault-parallel trenches that exposed an offset channel. These trenches provide further information about the timing and displacement of earthquakes on the Peninsula segment.

2.0 PREVIOUS WORK

2.1 1906 Earthquake

The Lawson report (Lawson, 1908), which documents surface displacements that occurred along the San Andreas fault during the 1906 earthquake, reports offsets to the north and south of the Crystal Springs South site. The nearest site to the north is at the causeway between Upper and Lower Crystal Springs reservoirs, about 4.7 km northwest of the site. The offset of the causeway was reported to be 8 ft (about 2.4 m). To the south, between Woodside and Portola Valley, about 9 km southeast of the site, J.C. Branner observed two fences offset about 8 and 8.5 ft (about 2.4 and 2.7 m). In Portola Valley, farther south, the documented slip dropped considerably. Rows of prune trees were reported to be offset about 2 ft (0.6 m). Reassessment of the photographs of this site suggested the total offset was about 1.2 m (Hall et al., 2001).

2.2 Paleoseismic Studies

The North Coast and Santa Cruz segments of the San Andreas fault each have paleoseismic sites that have yielded multi-event paleoseismic records; however, the Peninsula segment has seen only limited work to date, none of which, unfortunately, has yielded a robust history.

The nearest paleoseismic site to the Crystal Springs South site is at the Filoli estate, about 0.5 km to the southeast (Figure 3). At the Filoli site, Hall et al. (1999) excavated numerous fault-perpendicular and fault-parallel trenches where Spring Creek had breached the San Andreas fault scarp and deposited late Holocene alluvial fan materials over the fault. They obtained the currently accepted best estimate for Holocene slip rate on this segment, 17±4 mm/yr, from the 30±2 m offset of the thalweg of a channel dated to 2070±120 BP.

Efforts to develop a robust event chronology at the Filoli site were relatively unsuccessful due to the coarse and discontinuous nature of the channel deposits. Hall et al. (1999) do, however, infer the occurrence of two late Holocene earthquakes from a series of channels. The youngest suite of nested channels was offset about 2.5 m, which they conclude occurred during the 1906 earthquake because of its similarity in slip to that measured nearby following the event. A second set of nested channels was found deeper in the section. Hall et al. (1999) cut back the fault-parallel trench walls to within a few meters of the fault and projected the channels into the fault on either side. Based on their projections, they conclude the older channel sequence was offset about 4.1±0.5 m. The channel deposits were dated to 330±200 BP (1476-1647 AD calendar age). Because this offset was greater than the offset of the youngest channel sequence, they infer that that this set of channels had been offset in the 1906 and the penultimate earthquakes and, thus, that the penultimate earthquake occurred after 330±200 BP. Furthermore, because the estimated offset of about 1.6 ± 0.7 m in that event was smaller than the ca. 2.5 m that occurred in 1906, they conclude that the earthquake was likely generated by rupture of a shorter section of fault than in 1906, perhaps only the Peninsula segment, and probably had a magnitude of about **M** 7.0-7.4. They suggest, based on the poorly constrained age of the event and their inferences regarding rupture length, that the 1838 earthquake, which occurred on the peninsula, is a candidate for the event. The channel offset data; however, allow alternative interpretations, including that there is no additional offset of the older channel and that no pre-1906 event is required to explain the data at the site (Zachariasen et al., 2010; 2011).

Hall et al. (1999) also speculate on the occurrence of a third event. The older channel sequence described above, which crossed the fault at high angle, looped back and ran along the fault for about 25 m. They

suggest that a stream is most likely to begin following a fault immediately after a surface rupturing event. Thus, they speculate that the prior event occurred shortly before the age of deposition of the channel deposits and that, therefore, the age of the third event was during or shortly after ca. 1467-1647 AD. Again, however, this is speculative, and their study provides no direct evidence of a third event at Filoli.

In recent years, further paleoseismic efforts have been directed towards the Peninsula segment, which have produced mixed results. Prentice and Moreno (2007) excavated a trench in alluvial fan deposits at the north end of Crystal Springs reservoir, about 10 km northwest of the Crystal Springs South site, and identified the 1906 rupture and one prior event. The age of the prior event was not reported but the absence of European pollen in sediments bracketing the event horizon suggests the event predates the 1820 European settlement. More recent age constraints suggest the event occurred between AD 890-1260 (Prentice et al., 2008). Another trench at Crystal Springs reservoir exposed evidence of the 1906 earthquake but no earlier events in the upper 3 m (since ca. AD 1130 [Prentice et al., 2008; C. Prentice, pers. comm., 2008]). Prentice et al. (2008) suggest possible explanations for these observations including (1) that all exposed deposits postdate the penultimate event because of high sedimentation rates; (2) a long elapsed time between earthquakes, or (3) the event horizon represents multiple earthquakes, not just 1906.

Baldwin et al. (2006) and Baldwin and Prentice (2008) report evidence of two or three pre-1906 events in about 1000 years exposed in a trench at Portola Valley Town Center. These events have been interpreted from warped marsh/fluvial and colluvial wedge stratigraphy. The interpretation includes events occurring at: A.D. 1030 to 1490, A.D. 1260 to 1490, and 1906; interpreting the second event as two events (AD 1260-1490 and AD 1410 to 1640) is also permitted by the data (Baldwin and Prentice, 2008). The stratigraphy is complicated and the results depend on preservation of per-event colluvial wedges, which may or may not be reflected in a complete earthquake record. Evidence for an 1838 event was not found, but the resolution is not sufficient to rule it out.

The penultimate event identified at Grizzly Flat, on the Santa Cruz mountains section (SAS), southeast of the Peninsula segment, has been dated to AD 1630-1660 (or 1600-1670; Schwartz et al., 1998); the penultimate event at Vedanta, on SAN, northwest of the Peninsula, occurred between AD 1670 and 1740 (Zhang et al., 2006). The similarity in penultimate event ages at these sites, and also Bolinas Lagoon (Knudsen et al., 2002), has been used to support a full-fault rupture interpretation for the penultimate event on the northern San Andreas fault (Schwartz et al., 1998). Conversely, these could be independent smaller events closely spaced in time. WGCEP (2003, 2008) preferred the former model. Determining the age of the penultimate and earlier events on the Peninsula segment would be significant in evaluating the two models.

Recent paleoseismic investigations by Streig et al. (2014) along the SAS at Hazel Dell reveal evidence for four surface rupturing events, the 1906 rupture and three prior events. Historical constraints from interpreted cut wood chips recovered during trenching suggest an age constraint of 1840-1890 for the penultimate event, and 1815-1895 for the antepenultimate event; the oldest event is constrained between 760-1318. Streig et al. (2014) correlate their penultimate event to the historic 1890 earthquake, and their antepenultimate event to the historic 1838 earthquake, estimated as M6 and M7.2, respectively. Data from these investigations suggest more frequent surface rupturing events than previously identified on the SAS and more frequent than on the Peninsula section (Streig et al., 2014; Zachariasen et al., 2011).

3.0 CRYSTAL SPRINGS SOUTH (CSS) SITE

3.1 Setting

This study presents the results of a trenching investigation of the CSS paleoseismic site, between Filoli and Crystal Springs reservoir (Figures 2-4). The site is in the San Francisco Public Utilities Commission (SFPUC) Peninsula Watershed. We selected the site using the UNAVCO Plate Boundary Observatory Earthscope LiDAR data, acquired along the full length of the northern San Andreas fault (Figure 4).[1] At this site, the San Andreas fault runs along the eastern edge of the Santa Cruz mountains, along the western edge of the fault-controlled San Andreas "rift" valley. The fault here has a component of west-side-up vertical displacement, which has led to the formation of a 5-10 m-high scarp along the foot of the mountains. The setting is similar to that of the Filoli site, in that Holocene sedimentation has been dominated by deposition of alluvial deposits from Spring Creek. The creek, which is currently entrenched to the south of the site, breached the scarp and deposited alluvium across and east of the fault. The fault here strikes about N35W. We selected the CSS site where the main fault scarp has been eroded back, leaving the fault itself outboard of the eroded scarp and buried by young alluvial deposits from Spring Creek. A small Holocene scarp is evident in the LiDAR data and on the ground, just north of the intersection of Old Cañada Road and a small spur road heading northeast (Figures 4 and 5).

Trench T1 and T2 were excavated as part of the first phase of investigations (Figure 6; Zachariasen et al., 2011). Trench T1 was excavated across the Holocene scarp; trench T2 is located to the southeast, on the south side of the spur road, on strike with the Holocene scarp but where the fault is buried and no scarp is readily evident in the Lidar or on the ground (Figure 4). In this phase of the study, we excavated four additional trenches. Trench T3 was excavated east of the fault zone connecting the eastern ends of trenches T1 and T2. Trench T4 was excavated as a fault-parallel trench west of the SAF. Another fault parallel trench, T5, was excavated between T3 and the fault zone. T5b is a further fault parallel excavation extending the western wall of T5 closer to the fault zone. The purpose of excavating the fault-parallel trenches was to trace a buried fluvial channel first recognized in trench T1. Trench T6 was excavated as confirmatory fault perpendicular trench between T2 and the fault parallel trenches (Figure 5).

3.2 Methods

The trenches were excavated with a rubber-tire backhoe with a 3-foot-wide bucket and shored with 7-foot-long aluminum hydraulic speed shores. Topsoil was stored separately from the remaining spoil, which was covered with tarps. All spoils were stored on plywood sheets in order to minimize impact to the ground surface, and a wildlife exclusion fence was erected around each trench. Biological, cultural, and Native American monitors provided by the SFPUC over saw the excavation. The trench walls were manually scraped and cleaned, then gridded with a 1- by 0.5 m string grid. In order to establish a uniform and consistent stratigraphy for the entire site fault parallel and perpendicular trench excavations were intersected and horizons were cross correlated. We produced sketch logs of each wall on mylar graph paper at 1:20 scale. We photographed each grid square and created rectified photomosaics of each wall in Adobe Photoshop. We logged the trench walls at scales of 1:15 (T1), 1:12 (T2), and 1:10 (T3-T6). We collected charcoal samples for radiocarbon dating as well as bulk soil samples and samples for pollen analysis.

---

[1] *This material is based on services provided to the Plate Boundary Observatory by NCALM (http://www.ncalm.org). PBO is operated by UNAVCO for EarthScope (http://www.earthscope.org) and supported by the National Science Foundation (No. EAR-0350028 and EAR-0732947). This material is provided by the OpenTopography Facility (http://www.opentopography.org) with support from the National Science Foundation under NSF Award Numbers 0930731 & 093064.*

3.3 Trench Stratigraphy

All trenches exposed fluvial channel and overbank deposits that overlie a dark grey clayey deposit that contains completely weathered pebble-sized clasts; this is the deepest deposit exposed in the trenches and is likely older, highly weathered colluvium. The overlying fluvial deposits are cut by two distinct generations of faults. The younger set of faults break nearly to the ground surface, and we interpret these to represent 1906 surface faulting that has been buried by post-1906 sediments. The older faults terminate below colluvial rubble derived from faulted gravel deposits. For completeness of the findings from Crystal Springs South Trench Site we include a summary of findings from the previous phase (Trenches T1 and T2) as well (for a more complete description, see Zachariasen et al., 2011). Descriptions of each trench follow.

3.3.1 Cross-fault Trenches

Trench T2

Stratigraphic and faulting relationships are clearest in trench T2, especially the south wall (Figures 7a and 7b). The trench was excavated northeast-southwest, across and orthogonal to the southeastward projection of the Holocene scarp observed north of the spur road (Figure 5). The trench was about 8 meters long and 2-2.5 m deep. The depth was limited by the presence of ground water, which was somewhat shallower on the west side of the fault. The fault zone is located between meters 4 and 6 in the trench.

The trench exposed a suite of fluvial deposits overlying old weathered colluvium (unit 100). The basal unit was evident from about 1 m above the trench floor on the west side of the fault. On the east side it was at or just below the floor of the trench. It is light to dark grey, often with orange mottling, sandy silty clay to clayey sand.

Fluvial deposits overlie the basal colluvium. The upper contact of the colluvium is generally eroded and scoured, suggesting the stream removed an unknown amount of the colluvium prior to depositing the alluvium. We have divided the fluvial deposits into stratigraphic packages based on the relative amounts of fine vs. coarse-grained materials reflecting dominant depositional energy level, but each distinct package contains numerous lenses of material with different grain sizes, and many of the contacts are gradational. Directly overlying the weathered colluvium is a clast-supported granule to cobble gravel in a dry, loose sand to granule matrix (unit 60). Unit 60 is about 20 cm thick at the western end of the trench but deepens into a channel of greater than a meter thickness. The fault cuts the channel where it is thickest. Unit 60 is present on both sides of the fault.

Above the gravel deposit is a fine-grained overbank deposit of sand and silt (Unit 40), with several gravel lenses. This unit is present along the full length of the trench. Within the fault zone, we have subdivided unit 40 into smaller subunits, which are not readily evident outside the fault zone. A well-sorted, matrix- to clast-supported gravel (Unit 25) overlies the unit 40 silt on the eastern, downthrown, side of the fault only. The uppermost deposits (units 20 and 10) in the trench comprise heavily bioturbated yellow-brown, hard, dry, massive pebbly sandy silt. The uppermost part of this (unit 10) includes the modern A-horizon.

An unsorted, unbedded, chaotic, pebble to cobble gravel with abundant silt and sand A (unit “R”) is found between subunits of unit 40. We interpret this to be a colluvial wedge of rubble derived from unit 60, which was exposed during faulting, providing a source for the gravel. A classical wedge shape is evident on the south wall exposure (Figure 7a); on the north wall (Figure 7b), the wedge is not as clear and the

material appears as an irregularly shaped deposit of rubble, discussed below.

Event Stratigraphy

The fault zone in trench T2 includes evidence of two distinct events. The youngest event is represented by the faults that reach highest in the section; these are marked in red in Figures 7a and 7b. This younger generation of faults, which occur on either edge of the fault zone, terminate within the bioturbated material near the top of the trench (unit 20). Because of the bioturbation, the exact termination has been obscured. We interpret these faults to represent traces of the 1906 rupture.

A second event, which we call "Event G", is evident in the stratigraphy and is represented by purple colored faults in Figures 7a and 7b. The scarp-derived colluvium “R” occurs within the fine overbank deposits of Unit 40. It overlies faulted overbank deposits (Unit 40, subunit A in the southeast wall [Figure 7a] and subunit b in the northwest wall [Figure 7b])), which constituted the ground surface at the time of the older earthquake (Event G on Figure 7a). The scarp-derived colluvium is in turn overlain by more fine-grained material. We interpret the stratigraphy to indicate that the earlier event occurred when Unit 40 was at the ground surface and overbank silts were being deposited. Because only the lower part of Unit 40 had been deposited at the time of the event, the underlying gravel (Unit 60) was exposed in the scarp. Gravel fell from the exposed scarp and was deposited on the overbank sands and silts of lower Unit 40 (subunit A, silty sand). The fluvial environment did not change significantly following the event, and silt overbank deposition continued (unit A', fine silty sand, the post-event deposit is similar to A, the pre-event deposit, though slightly finer. Thus, the colluvial wedge from the penultimate event is preserved between earlier and later Unit 40 overbank deposits. These relationships are well expressed in the south wall of the trench (Figure 7a). In the north wall (Figure 7b), the relationships are less clear, in part because the younger (1906?) event faulted through the older fault zone and colluvium. Rubble from the penultimate colluvium has been drawn into the fault zone of the 1906 event, overprinting the earlier event and leaving the stratigraphic and faulting relationships less clear.

There is no evidence in the trench for any other event since the start of deposition of the fluvial deposits that overlie the dark basal clay-rich material.

Trench T1

Trench T1 trends northeast, orthogonal to the fault and was excavated across the small west-side-up scarp evident in the Lidar and on the ground. The trench is about 12 meters long and 2-2.5 m deep. The fault zone is below the scarp, between meters 6 and 8. The east side is downthrown relative to the west side. The log of the north wall of the trench is shown in Figure 8.

The stratigraphy in Trench T1 is broadly similar to that in Trench T2. The same grey clay-rich weathered colluvium (unit 100) forms the basal unit. Overlying the unit 100 basal colluvium is a series of fluvial deposits consisting of gravel, sand, and silt. These are similar in appearance and provenance to those in trench T2, but individual units do not correlate between trenches (i.e. numbered units in T1 are not necessarily the same unit as identically numbered units in T2). On the east side of the fault, dry, loose, poorly sorted, pebble-cobble gravel (unit 70) overlies the basal clay-rich weathered colluvium (unit 100?). Above this gravel, the stratigraphy consists of interfingering gravel and silty sand lenses. Massive to lightly bedded, yellow-brown sandy silt to silty sand, with lenses of coarse sand and fine gravel (unit 60) overlies unit 70 only on the east side of the fault. Above this finer unit is another gravel, unit 50, which consists of a dry, loose, massive to crudely bedded, pebble-cobble gravel, with a coarse sand to granule matrix.

On the west side of the fault, a dry, loose, coarse poorly sorted sandy pebble-cobble gravel (unit 70?) directly overlies unit 100. Although the clasts are larger, we consider that this gravel probably correlates approximately with the unit 70 gravel east of the fault. Another dry, loose, yellow-brown, poorly sorted, massive to crudely horizontally bedded, pebble gravel (Unit 50?) directly overlies the coarse gravel.

The gravel on the west side of the fault has well-developed channel morphology and has cut into the underlying deposits, thickening abruptly near meter 4. This thick channel deposit has been cut by the fault at meter 6 and is not evident on the east side of the fault, although the unit 50 gravels are still present. Although the gravels may correlate across the fault, the channel on the east side has been faulted southeastwards and is no longer present at the trench location. The channel edge trends obliquely to the trench, and the channel appears to have flowed in a north-northeast direction.

A highly bioturbated, yellow-brown, massive, pebbly sandy silt, with abundant roots, charcoal, and krotovina (unit 40) overlies the gravel. This is topped by the modern "A" horizon topsoil.

Within the fault zone, units are hard to identify with certainty due to the shearing and disruption from faulting, but the general stratigraphy is apparent, with pockets of gravel and sandy silt tentatively associated with the major units defined outside the fault zone, except where very strongly sheared (e.g. within fault zone between meters 7 and 8). We have defined two other units within the fault zone. Unit F_G is chaotic pebble-cobble gravel that we interpret as fissure fill formed in response to the penultimate event (discussed below) and subsequently faulted in the most recent event. R_{1906} is a loose cobble gravel with sand-pebble matrix that we interpret as colluvium formed after the most recent (1906?) event from the raveling of exposed gravel from the free face formed in that event.

Event Stratigraphy

The event stratigraphy in Trench T1 reveals a similar history to that in Trench T2, with evidence of two events since the deposition of the fluvial deposits overlying the basal weathered colluvium. The most recent event, which we assume was the 1906 earthquake, ruptured to near the current ground surface. Traces in the south wall extend to within about 20 cm of the top of unit 40 where they become indistinct within a large krotovina. In the north wall, the 1906 traces (red in Figure 8) extend well into unit 40 and are overlain by colluvial rubble raveled off the scarp free face.

The second event back ("Event G") occurred when only the lower part of the unit 40 sandy silt had been deposited and was at the ground surface. The fault traces associated with this event are shown in pink in Figure 8 in a zone about a meter wide located east of the 1906 traces. Two traces at the eastern edge of this zone, at about meter 7.5, cut through the gravel units and into the base of the overlying overbank silts, bounding a sheared zone of mixed coarse and fine material. These traces are overlain by a line of gravel clasts (large pebble to small cobble size) within the silt unit that we interpret to be rubble that raveled off the gravel exposed during the event. Event G also produced a fissure (F_G) or colluvial rubble package filled with chaotic cobble gravel in a silty sand matrix. The 1906 event subsequently faulted the fissure rubble, and deposited the colluvial rubble (R_{1906}) after the event.

There is no evidence in the trench for any other event since the start of deposition of the fluvial deposits that overlie the dark basal clay.

Trench T6

Trench T6 trends northeast-southwest, approximately 4 m north of T2 and was excavated perpendicular to the fault. The trench is about 8 m long and 2.25 m deep. The eastern end of T6 intersects with the western

wall of fault parallel trench T3 (Figures 5 and 9). The fault zone is below the scarp, between meters 3 and 6, with the east side downthrown relative to the west side. The logs of the trench are shown in Figure 10.

Trench T6 exposed essentially the same stratigraphic packages as trench T2. Unit 100 colluvium lies at the base of the trench and is overlain by a series of fluvial deposits, including interfingering gravel, sand, and silt. These units include: unit 20, brown, strongly bioturbated sandy silt with gravel; unit 25, a fluvial channel gravel, present only on the east side of the fault and comprising dark grayish brown, rounded sandy gravel; unit 40, brown sandy silt with pebble gravel lenses constituting fluvial overbank deposits. Unit 60 overlies the unit 100 colluvium. In T2, unit 60 consisted almost entirely of gravel. In T6, on the west side of the fault, this is also the case. However, on the east side of the fault, the material between unit 100 and the silt of unit 40 consists of interbedded gravel and silty sand lenses; we include it all in unit 60.

Event Stratigraphy

Trench T6 exposed evidence for two surface rupturing earthquakes. The most recent fault rupture, presumably 1906, is reflected in faulting concentrated between meters 3 and 4 that extends into the bioturbated sandy silt that constitutes unit 20 (Figure 10). The full upward extension of these faults was not clear due to significant near-surface bioturbation. An older surface rupture is identified by a series of upward fault truncations at the basal contact of a gravel unit U25 between meters 4.5 and 5.5 at approximately 0.5-1 m below ground surface. The stratigraphy here differs from T2 in that no unfaulted silt is present between the penultimate fault traces and the overlying gravel, presumably reflecting a lateral variation in deposition following the event. This penultimate event is exposed on both walls. On the north wall at meter 3.6, approximately 75cm below ground surface, a single fault strand offsets the basal contact of unit U40 and terminates within this unit. This could represent a third event back, but the support for such an event is weak. This relationship is not present in the south wall, nor in any other exposure at the site.

3.3.2 Fault-parallel trenches

As described above, trench T1 exposed a distinctive channel deposit west of the fault. The channel trends towards and is offset by the fault. We excavated a series of fault-parallel trenches in order to track this channel on both sides of the fault to determine the magnitude of displacement that has occurred across the fault since abandonment of this channel.

Trench T3

Trench T3 trends northwest-southeast and was excavated parallel to and east of the fault zone (Figure 5). The trench is about 18.5 m long and approximately 2.5 m deep. The northwestern end of T3 intersects the northeastern end of T1, and the southeastern end of T3 intersects the northeastern end of T2. T3 was excavated to trace, on the northeast side of the fault, the buried channel that was first exposed in trench T1 on the southwestern side. The log of trench T3 is shown in Figure 11.

The buried channel is expressed by a high energy fluvial deposit composed of rounded to sub-rounded gravel to boulder-sized clasts deposited within series of stacked channel incisions concentrated between meters 9 and 13 (3 to 5 m wide). This channel complex is distinctive within stratigraphic section exposed at the CSS site. It incised into otherwise horizontally continuous finer grained deposits identified as units 10-90. The oldest unit exposed in our trenches incised by the buried channel is Unit 100.

Trench T4

Trench T4 trends northwest-southeast and was excavated parallel to the fault zone on the west side. The

trench is about 18 m long and approximately 2 m deep. Trench T4 intersects T1 between meters 12-13.5 and 3-4.5, in the east and west walls, respectively. The southeastern end of T4 is 1 m northeast of northeastern wall of T2. T4 was excavated to trace the same buried channel that crosses the fault zone and that was exposed in trenches T1 and T3. The log of the trench is shown in Figure 12.

As in T3, the channel is unique within the section and easily identifiable. The channel margins were located between about meters 10 and 14 (~4m wide). The intersection of the two trenches occurs within the channel.

Trench T5 and T5b

Trench T5 trends northwest-southeast and was excavated parallel to and east of the fault zone, between the fault and trench T3 (Figures 5 and 9). The trench is about 7.5 m long and approximately 2.5 m deep. The northwestern end of T5 is 3 m southeast of T1and southeastern end is 2.5 m northeast of T2. The eastern wall of T5 is 0.5-0.75 m northwest of T3 and 0.5-1.2 m southeast of the fault zone. The log of the trench is shown in Figure 13.

Trench T5 was excavated to trace the buried fluvial channel between the fault zone and T3. The buried fluvial channel margins were exposed between about meters 9 and 12. After the western wall of T5 was logged, we excavated it farther back towards the fault zone (T5b) in order to expose the buried channel closer to the fault zone. The T5b exposure reveals the channel in contact with the fault, which intersects the channel at about meter 12.5 (Figure 13).

3.4 Age Constraints

We obtained both detrital charcoal and bulk samples from throughout the section exposed in each trench and submitted several for dating. Macrofloral remains from bulk samples were extracted by PaleoResearch Lab and only identified macrofloral fragments were dated. These fragile samples were likely not transported long distances, suggesting minimal inheritance and tighter constraints on the age of the deposit. The samples were analyzed by accelerator mass spectrometry (AMS) at Lawrence Livermore National Laboratory for radiocarbon age dating. The OxCal program (version 4.2.4) (Bronk-Ramsey 2008, 2009; Bronk-Ramsey and Lee, 2013; Reimer et al. 2004a, 2004b, 2013) was used to determine the calibrated calendar age for each radiocarbon sample. Stratigraphic models were developed for Event G and the offset channel, and the ages for these horizons were calibrated in OxCal using these models.

The trench logs show the sample locations, and the age data are summarized in Table 1. We dated samples from a variety of horizons but concentrated the dating on samples above and below the event G horizon in the south wall of Trench 2 (Figure 14) and around the offset buried channel in trenches T3 and T4. In the following discussion, all dates are rounded to the nearest decade.

In the first phase of the project, we dated one sample (T1N-5) from the basal weathered colluvial unit 100, which had a calibrated calendar date of 1220-1020 BCE, leading us to interpret the basal colluvium as much older than other samples. However, samples from this colluvium obtained from trenches dug as part of this second phase (T3E-C63 and bulk sample B9 from T3W) yield much younger calibrated ages (780-9804 cal AD and 430-570 cal AD, respectively), indicating that the basal colluvium may have been deposited only shortly before the rest of the sequence.

Trench T2 exposed faulting relationships that constrain Event G to have occurred between the deposition of a silt bed (unit 40) and the deposition of a colluvial wedge overlying the silt. Eight samples pre-dating the event horizon from the pre-event silt below the colluvial wedge in the southeast wall of Trench T2 and

five samples post-dating the event horizon from the unit 40 silt that overlies the colluvial wedge that formed after Event G were dated and used in the OxCal age model (Figure 15). More samples from this and other trenches were also collected and dated, but the preliminary stratigraphic model we have used is limited to detrital charcoal ages from trench T2, where faulting stratigraphy is best expressed. The model yields a tightly constrained age for Event G of 990-1020 cal AD. Further analysis using more samples may ultimately adjust this age.

We also collected detrital charcoal and bulk samples and dated 18 samples to determine the age of the offset buried fluvial channel. The OxCal analysis indicates that the channel deposits were emplaced between 790-880 cal AD (min) and 1100-1150 cal AD (max) (Figure 15). This age range overlaps the age range of event G, suggesting the event occurred shortly after channel abandonment.

3.5 Fault Displacement

The channel exposed in trenches T1, T3, T4 and T5 has been offset across the fault. The fault-parallel trenches were excavated to expose the channel and track it into the fault zone from either side to document the amount of displacement that has occurred on the fault since abandonment of the channel. We recorded the location of the margins of the channel where they projected to the ground surface. Figure 16 shows the location of the channel margins, marked by pink dots, relative to the trenches and the fault zone. The channel trends northeast, nearly orthogonal to the orientation of trenches T3, T4 and T5. The green dots show the preferred restoration of the channel on the eastern side to match that on the western side, a restoration of about 7 m. A number of factors introduce uncertainty into the magnitude of the slip restoration. The limited number of exposures of the channel on the west side of the fault, two points on either margin, mean that the orientation of the channel is not as well constrained as that on the east side, with five exposures per side and where we were able to extend our exposure right to the fault zone, even intersecting it in T5b. In addition, the fault zone is about 2-m wide, allowing for some uncertainty in the precise projection of the channel at the point of displacement. Nevertheless, using a range of alternative projections, we find that the offset recorded by the channel is between 6 and 8 m.

4.0 DISCUSSION

The CSS trenches exposed a suite of fluvial deposits that are younger than the weathered colluvium (unit 100) exposed at the base of trenches T1, T2, and T6. Overlying deposits, up to the heavily bioturbated uppermost half-meter, appear to have been deposited within a few hundred years, between about 800 and 1500 AD. The distinctive channel deposit within the sequence, exposed in several trenches and dated to 790-1150 cal AD, formed in a channel that flowed across the fault. Following abandonment of the channel, the preserved deposit was cut by and offset across the fault.

Only two faulting events have been identified in the trenches. We assume the most recent earthquake recorded in the section is the 1906 earthquake. The older event, recognized by the upward termination of numerous faults strand overlain by a colluvial wedge, occurred at 990-1020 cal AD. The channel deposits, except perhaps the youngest, have been affected by both events, thus constraining the age of the offset channel to be older than the age of offset, i.e. older than 1020 AD.

The margins of channel deposits observed in several fault-parallel exposures on either side of the fault mark out the location of the offset paleochannel. The channel flowed northeast, across the fault. Reconstruction of the channel indicates that it has been offset 6-8 m since its abandonment. The nearest offset measurement following the 1906 earthquake was obtained about 11 km northwest of the CSS site and was recorded as 2.7 m (Lawson, 1908). Assuming a similar amount of slip occurred at the CSS site in 1906, it leaves 3.3-5.3 m of slip to have occurred between abandonment of the channel and 1906. That amount of offset is consistent with one or two 1906-size earthquakes. Thus, it is consistent with the two events observed in the trenches since abandonment of the channel at about 1020 AD. It is also permissive of an additional 1906-size or smaller event in that time period that has not been recognized in the CSS trenches, obscured perhaps in the heavily bioturbated section above the event G horizon. It is not, however, consistent with many more additional events of comparable magnitude.

The slip rate over the last 2000 years measured at Filoli is 17±4 mm/yr (Hall et al, 1999). Over the ~1020 years since the channel was abandoned, at that slip rate, about 17 m of slip should have accumulated on the fault. The fact that only 6-8 m of slip has occurred in that time suggests a significant slip deficit on the fault. This, in turn, suggests that either the slip rate has been irregular in the late Holocene, or alternatively that some fraction of the total slip rate is occurring off the 1906 trace in this area. As seen in Figure 4, other traces of the fault have been mapped on either side of the 1906 trace. These do not have as pronounced geomorphic expression as the 1906 trace, but are mapped as late Quaternary.

The data from these trenches suggest that the penultimate event on this part of the San Andreas fault may have occurred as many as 900 years before the 1906 event. Even if an additional, unrecognized event has occurred here, these results still suggest a recurrence interval on the order of several hundred years. That is somewhat consistent with the recurrence suggested at other paleoseismic sites on the Peninsula. At the Crystal Springs site, north of the reservoir, Prentice et al. (2008) found only one pre-1906 event dated about 1000 years ago. At Portola Valley, Baldwin and Prentice (2008) report 3-4 events in the past ~1000 years. At the Scarp Creek site, 0.5 km southwest of the CSS site, Prentice et al. (2014) have identified three events in about 900 years. At Filoli, Hall et al. (1999) interpret a sequence of nested channels as indicating that three events have occurred within the past ~500 years, a somewhat more frequent recurrence. As Zachariasen et al. (2011), note; however, the Filoli data can also be interpreted to indicate only a single event in that time period.

The results from most of these sites, which suggest that 2-4 events have occurred on the Peninsula section of the fault in the past ca. 1000 years, however, differ markedly from the paleoseismic record at the Mill Canyon-Arano Flat site on the Santa Cruz Mountains segment of the San Andreas fault, where Fumal et

al. (2003) find evidence of nine events in about 1000 years. They also seem to differ from the record at the Hazel Dell site, on the Santa Cruz Mountains segment about 10 km northeast of Arano Flat, where evidence of two 19th-century earthquakes in addition to the 1906 earthquake was identified. (Figure 1; Streig et al., 2014).

If it is correct that the history of fault rupture on the Peninsula (SAP) is one of longer recurrence intervals than in the Santa Cruz Mountains (SAS), it suggests that models in which the entire northern San Andreas ruptures together in 1906-like events, or that the Peninsula most often ruptures in conjunction with the Santa Cruz Mountains section, may not be the best or most representative of the fault rupture behavior. Furthermore, the segmentation model that formed the basis of most of the past few statewide seismic hazard models in general may be incorrect. Paleoseismic data from sites to the south (Arano Flat-Mill Canyon, Hazel Dell, and Portola Valley) suggest increasing average recurrence interval northward, with Arano Flat having a much shorter interval than the other two sites, which are in turn shorter than the last interval at CSS. This suggests that the model of segmentation, in which the fault is divided into a small number of long-lived segments that rupture characteristically, either with other segments or alone, is perhaps not representative behavior of the SAF. The UCERF3 model, which permits greater spatial and temporal variability in rupture patterns than did prior models, even if still favoring larger segment ruptures, may be more representative.

As at the Crystal Springs, Portola Valley, and Scarp Creek sites, there is as yet no indication of an event in 1838 at CSS. The offset channel data allow an additional event besides 1906 and event G, and an 1838 earthquake rupture could be unrecognized within the uppermost bioturbated zone, but there is no positive evidence for it. To date, the only geologic evidence that has been found to support the 1838 event on the San Andreas fault is an offset 330 BP-aged channel at Filoli interpreted by Hall et al. (1999) as possibly offset during the 1838 earthquake. Yet, theirs is just one possible interpretation of the data. Zachariasen et al. (2010) reanalyzed the Hall et al. (1999) offset data and concluded that, whereas their channel reconstruction was a plausible one, equally plausible reconstructions would allow greater or lesser amounts of offset, beyond their stated uncertainties. Based on that reassessment, Zachariasen et al. (2010) concluded that the data can be interpreted to indicate that the older channel was offset by only a single event, 1906. The paleoseismic results at Peninsula sites to date are largely permissive of an 1838 event, but none of them shows clear evidence of such an event.

5.0 CONCLUSIONS

The CSS paleoseismic site has provided documentation in three cross-fault trenches of two earthquake events occurring within the past 1000 years. In addition, a buried channel exposed in several trenches on both sides of the fault has proven to be a good strain gauge for determining displacement.

Reconstruction of the channel indicates that total offset of this ca. ~1000-yr old channel has been about 6-8 m. The offset in 1906, measured 11 km northwest of the CSS site, was about 2.7 m, suggesting that the event history as preserved in the trench is largely complete, and only two or three 1906-sized events could have occurred at the CSS site within the last ca. 1000 yrs. The average recurrence interval is thus on the order of 300-500 years, in contrast to the 100-yr interval suggested at Arano Flat on the Santa Cruz Mountains section. These results suggest that the Peninsula Section of the SAF accrues and releases stress differently than to the south, specifically Santa Cruz Mountains Segment.

The slip rate over the last 2000 years measured at Filoli is 17±4 mm/yr (Hall et al, 1999). Over 900 years, at that slip rate, about two to three times as much slip should have accumulated on the fault as is documented at the CSS site, suggesting a slip deficit on the fault. This suggests that either other fault traces accommodate appreciable slip without preserving significant geomorphic expressions or slip rates vary on thousand-year timescales.

The Peninsula section of the San Andreas fault ruptured in the 1906 San Francisco earthquake, but it is unclear when the penultimate event occurred. The 1838 earthquake has been proposed as a San Andreas event, but no direct paleoseismic evidence of that event has been found to date. The Crystal Springs South paleoseismic data do not provide that evidence. There is no indication of an 1838 event, nor of any other event, between 1906 and 1000 AD, although bioturbation or a depositional hiatus could obscure evidence of a younger event. The absence of evidence for an 1838 event; however, is consistent with results from Crystal Springs, Portola Valley, and Scarp Creek paleoseismic sites. For now, the 1838 earthquake occurring on the Peninsula section of the SAF must remain speculative.

6.0 ACKNOWLEDGMENTS

Appreciation goes to the City and County of San Francisco and the Natural Resources and Lands Management Division of the San Francisco Public Utilities Commission for giving permission to work at the site in the watershed and providing biological and cultural monitoring services for the excavation. Keith Dick of Keith's Excavating dug and backfilled the trenches for us. The field and office assistance provided by USGS interns, volunteers, and employees is greatly appreciated.

7.0 REFERENCES

Bakun, W.H., 1999, Seismic activity of the San Francisco Bay region, Bulletin of the Seismological Society of America; June 1999; v. 89; no. 3; p. 764-784.

Baldwin, J. and Prentice, C., 2008, Earthquake records of the Peninsula segment of the San Andreas fault, Portola Valley, California: Collaborative research with William Lettis & Associates, inc. and U.S. Geological Survey, Final Technical Report, U. S. Geological Survey National Earthquake Hazards Reduction Program Award Number 05HQGR0073.

Baldwin, J., Prentice, C., Wetenkamp, J., and Sundermann, S., 2006, Preliminary Earthquake Record of the Peninsula Section of the San Andreas fault, Portola Valley, California, Seismological Research Letters Volume 77, Number 2, p. 248.

Bronk Ramsey, C. (2009). Bayesian analysis of radiocarbon dates. Radiocarbon, 51(1), 337-360.

Bronk Ramsey, C. (2008). Deposition models for chronological records. Quaternary Science Reviews, 27(1-2), 42-60.

Bronk Ramsey, C., & Lee, S. (2013). Recent and Planned Developments of the Program OxCal. Radiocarbon, 55(2-3), 720-730. Fumal, T.E. Heingartner, G.F. Samrad, L., Dawson, T.E., Hamilton, J.C., and Baldwin, J.N., 2003, Photomosaics and Logs of Trenches on the San Andreas Fault at Arano Flat near Watsonville, California: U.S. Geological Survey Open-File Report 03-450, Version 1.0.

Hall, N.T., Wright, R.H., and, C.S. Prentice, 2001, Studies along the peninsula segment of the San Andreas fault, San Mateo and Santa Clara Counties, California *in* Ferriz, H., and Anderson, R., eds., Engineering Geology Practice in Northern California: California Division of Mines and Geology, Bulletin 210, Special Publication 12, p. 193 - 210.

Hall, N.T., Wright, R.H., and Clahan, K.B., 1999, Paleoseismic studies of the San Francisco peninsula segment of the San Andreas fault zone near Woodside, California: Journal of Geophysical Research, v. 104, no. B10, p. 23,215-23,236.

Hayward fault Paleoearthquake Group (HPEG) (J. J. Lienkaemper, D.P. Schwartz, K.I. Kelson, W.R. Lettis, G.D. Simpson , J.R. Southon, J.A. Wanket, P.L. Williams), 1999, Timing of Paleoearthquakes on the Northern Hayward Fault — Preliminary Evidence in El Cerrito, California, U. S. Geological Survey Open-File Report 99-318

Knudsen, K.L., Witter, R.C., Garrison-Laney, C.E., Baldwin, J.N., and Carver, G.A, 2002, Past earthquake-induced rapid subsidence along the northern San Andreas fault: A paleoseismological method for investigating strike-slip faults: Bulletin of the Seismological Society of America, v. 92, no. 7, p. 2612-2636.

Lawson, A.C., 1908, The earthquake of 1868; *in* A.C. Lawson, ed., the California earthquake of April 18, 1906: Report of the State Earthquake Investigation Commission (vol. 1): Carnegie Institute of Washington Publication 87.

Prentice, C. S.; Clahan, K.; Sickler, R. R.; Salin, A.; DeLong, S. B.; McDermott, R.; Pickering, A.; Baldwin, J. N., 2014, Paleoseismic Studies of the Peninsula San Andreas Fault at the Filoli Estate, Woodside, California, Abstract T41C-4664 presented at 2014 Fall Meeting, AGU, San Francisco, Calif., 15-19 Dec.

Prentice, C. S.; Zachariasen, J. A.; Kozaci, O.; Clahan, K.; Sickler, R. R.; Rosa, C. M.; Hassett, W.; Feigelson, L.; Haproff, P. J.; DeLong, S.; Perkins, A.; Brooks, B. A.; Delano, J.; Baldwin, J. N., 2013, Paleoseismic Studies of the Peninsula San Andreas Fault near Crystal Springs Reservoir, Woodside, California,

Abstract T43A-2620 presented at 2013 Fall Meeting, AGU, San Francisco, Calif., 9-13 Dec.

Prentice, C. S., Zachariasen, J., Kozacı, Ö., Sanquini, A., Wolf, E., Sickler, R., Feigelson, L., Crankshaw, I., Rosa, C., and Baldwin, J., 2012, Paleoseismic study of the San Andreas Fault at the Crystal Springs South site, San Mateo County, California, Seismological Research Letters Volume 82, Number 2, SSA Annual Meeting 17-19 April 2012, San Diego, California.

Prentice, C. and Moreno, X., 2007, Paleoseismic site on the Peninsula San Andreas fault near Crystal Springs Reservoir: Preliminary results, *Seismological Research Letters* Volume 78, No. 2, p.315.

Prentice, C.S., Sickler, R.S.; Hecker, S.; Schwartz, D.P., Brown, J., 2008, Preliminary results from a new paleoseismic site on the San Andreas fault near Crystal Springs Reservoir, San Francisco peninsula, California, , *Seismological Research Letters* Volume 79, No. 2, p.360.

Reimer, P. J., Baillie, M. G. L., Bard, E., Bayliss, A., Beck, J. W., Blackwell, P. G., Bronk Ramsey, C., Buck, C. E., Burr, G. S., Edwards, R. L., Friedrich, M., Grootes, P. M., Guilderson, T. P., Hajdas, I., Heaton, T. J., Hogg, A. G., Hughen, K. A., Kaiser, K. F., Kromer, B., McCormac, F. G., Manning, S. W., Reimer, R. W., Richards, D. A., Southon, J. R., Talamo, S., Turney, C. S. M., van der Plicht, J., & Weyhenmeyer, C. E., 2009, IntCal09 and Marine09 radiocarbon age calibration curves, 0-50,000 years cal BP, *Radiocarbon, 51*(4), p. 1111-1150.

Schwartz, D.P., Pantosti, D., Okumura, K., Powers, T.J., and Hamilton, J., 1998, Paleoseismic investigations in the Santa Cruz mountains, California: Implications for recurrence of large-magnitude earthquakes on the San Andreas fault: Journal of Geophysical Research, v. 103, no. B8, p. 17,985-18001.

Streig, A.R., T. E. Dawson and R. J. Weldon, II (2014), Paleoseismic Evidence of the 1890 and 1838 Earthquakes on the Santa Cruz Mountains Section of the San Andreas Fault, near Corralitos, California, Bull. Seismo. Soc. Am., v104, pp 285-300, DOI: 10.1785/0120130009

Toppozada, T.R., and Borchardt, G., 1998, Re-evaluation of the 1836 "Hayward Fault" earthquake and the 1838 San Andreas Fault earthquake: Seismological Society of America Bulletin, v. 88, p. 140-159.

U.S. Geological Survey and California Geological Survey (USGS/CGS), 2006, Quaternary fault and fold database for the United States, accessed June and July 2011, from USGS web site: http//earthquakes.usgs.gov/regional/qfaults/.

2007 Working Group on California Earthquake Probabilities (WGCEP), 2008, The Uniform California Earthquake Rupture Forecast, Version 2 (UCERF 2), USGS Open File Report 2007-1437, CGS Special Report 203, SCEC Contribution #1138, Version 1.0

Working Group on California Earthquake Probabilities ((WGCEP), 2003, Earthquake Probabilities in the San Francisco Bay Region: 2002–2031, USGS Open-File Report 03-214.

Working Group on California Earthquake Probabilities (WGCEP), 1988, Probabilities of large earthquakes occurring in California on the San Andreas fault, U.S. Geological Survey Open-File Report, p. 62.

Working Group on California Earthquake Probabilities (WGCEP), 1990, Probabilities of large earthquakes in the San Francisco Bay Region, California, U.S. Geological Survey Circular, p. 51.

Working Group on Northern California Earthquake Potential (WGNCEP), 1996, Database of potential sources for earthquakes larger than magnitude 6 in northern California: U. S. Geological Survey Open-File Report 96-705.

Zachariasen, J. A.; Prentice, C. S.; Kozaci, O.; Sickler, R. R.; Baldwin, J. N.; Sanquini, A.; Knudsen, K. L., 2010,

Paleoseismic Study on the Peninsula Section of the San Andreas Fault South of Crystal Springs Reservoir, San Mateo County, California, American Geophysical Union, Fall Meeting 2010, abstract #S21C-2048.

Zhang, H., Niemi, T., and Fumal T., 2006, A 3000-year record of earthquakes on the northern San Andreas fault at the Vedanta marsh site, Olema, California: Seismological Research Letters, v. 77, p. 176.

APPENDIX

Unit Descriptions for trenches T5 and T6

T5E

BFC Gravels with sand; 10YR 5/2 Grayish brown; 80% gravel, 20% sand; gravels are rounded – well-rounded, up to ~16cm in size, moderately sorted, some clast imbrication; contains sand lenses; clast supported; stiff, loose, dry; smooth and abrupt basal contact; FLUVIAL CHANNEL

U40 Sandy silt with pebbles; 10YR 4/4 Dark yellowish brown; <5% gravel, 30% sand, 65%silt; well-rounded pebbles up to 1cm; with fine sand; massive, well-sorted; rare rootlets; dry, stiff; wavy, abrupt lower contact; FLUVIAL OVERBANK

U60 Sandy gravel; 10YR 3/2 Very dark grayish brown; 80% gravel, 15% sand, <5% silt; well-sorted; well-rounded gravels up to 9cm; internal bedding made up of small pebbles; no roots; damp, stiff; wavy and gradual basal contact; FLUVIAL DEPOSIT

T5WB Fault Zone Units and Notes

1 Zone of sheared sandy gravel; many vertically oriented clasts

2 Silt overlying fine sand and underlying fine-medium sand; this is intact stratigraphy not fissure fill; depositional contact

3 Crude horizontal bedding in BFC terminates closer to the shear zone

4 Tan, medium sand with few pebbles juxtaposed against darker silt with fine sand

5 silt underlying fine-medium sand

6 The fault can be traced clearly up to this location. It possibly extends upward into U40 where possible 1906 strands terminate

7 Gravel lens within U20

8 Gravel (possibly U25 in T2)

9 Sandy pebbly gravel, distinct from 8; possible fault contact

10 Pebbly unsorted medium sand

11 Pod of gravel overlying U100

T6S at station 2.5m

U20 Sandy silt with gravels; 10YR 4/3 brown; 20% gravels, 50% silt, 30% sand; well-rounded gravels up to 5cm (oval to round); fine sand; hard to very hard consistency; massive, no clear bedding or sorting; heavily bioturbated, common krotovinas; wavy and gradational (over 5 cm) basal contact; SHEET WASH/COLLUVIUM

U40 Silty sand; 10YR 5/3 brown; <3% gravels, 40% sand, 57% silt; occasional well-rounded gravels up to 3.5cm; fine sand and silt; very hard to extremely hard consistency, massive; common bioturbation and roots; irregular and clear basal contact; FLUVIAL OVERBANK with some COLLUVIUM

U60 Gravels with sand; 10 YR 5/3 brown; 75% gravels, 20% sand, 5% silt; rounded to well-rounded cobbles of up to 10cm in length, fine to medium sand; stiff to very stiff, internal bedding and some clast imbrication, moderately to well-sorted; rare bioturbation mainly by roots; wavy and abrupt basal contact; FLUVIAL CHANNEL

U100 Fine sand with clay; 10YR 2/2 very dark brown with red and gray mottling; 65% sand, 20% clay, 10% silt, <5% gravel; well-rounded (<3cm) gravels, fine to medium sand; stiff, massive; there is a 5-10cm thick sandy gravel lens near the upper contact; damp (wet at the fault zones); basal contact is not exposed; FLUVIAL/DEBRIS FLOW

T6S at station 6m

U10 Silty, pebbly sand with gravels; 10YR 5/3 brown; sub-rounded to sub-angular clasts of up to 2cm; 10% gravel, 70% sand, 20% silt; modern soil development; platy-blocky, no clay films; wavy basal contact; up to 20 cm thick; A-HORIZON

U20 Sandy silt with gravels; 10YR 4/3 brown; 15% gravel, 50% silt, 35% sand, rounded to angular gravels of up to 3cm, fine sands and silt; abundant krotovinas and common roots; not sorted, massive; dry; irregular and gradational basal contact; FLUVIAL SHEET WASH

U25 Sandy gravel; 10YR 4/2 dark grayish brown; 65% gravel, 35% sand; rounded to well-rounded gravels of up to 10cm, fine-medium sand; abundant rootlets; poor sorting; FLUVIAL CHANNEL

U40 Sandy silt with pebbles; 10YR 4/3 brown; 5% gravel, 55% silt, 40% sand; occasional rounded gravels up to 6cm; come bioturbation; common charcoal; some paleosols; contains fluvial channel lenses with well-sorted, imbricated small-medium pebbles; the lower section of U40 is damp and has more organic material and more clay (10YR 3/3 dark brown); abrupt basal contact; FLUVIAL OVERBANK

U60 Sandy gravel; 10YR ¾ dark yellowish brown; 70% gravel, 25% sand, 5% silt; rounded to well-rounded gravels up to 9cm; well-developed bedding and sorting; some silty sand lenses; no roots or krotivinas; FLUVIAL CHANNEL

Table 1. Crystal Springs South Trench Site

Trench	LAB #	Sample Name	^{14}C age	±	Calibrated	Cal. Software
T1N	149043	2010 CSS 1N2	900	30	1039 AD - 1210 AD	Oxcal v4.2 95.4%
T1N	149044	2010 CSS 1N4	835	25	1164 AD - 1257 AD	Oxcal v4.2 95.4%
T1N	149045	2010 CSS 1N5	2930	30	1220 BC - 1025 BC	Oxcal v4.2 95.4%
T1N	149046	2010 CSS 1N6	1060	25	900 AD - 1023 AD	Oxcal v4.2 95.4%
T1S	149047	2010 CSS 1S2	960	25	1021 AD - 1155 AD	Oxcal v4.2 95.4%
T2N	149048	2010 CSS 2N1	1035	25	970 AD - 1031 AD	Oxcal v4.2 95.4%
T2S	149049	2010 CSS 2S2	5250	90	4328 BC - 3813 BC	Oxcal v4.2 95.4%
T2S	150346	T2S-78	1045	30	900 AD - 1030 AD	Oxcal v4.2 95.4%
T2S	149893	T2S-5	955	20	1022-1155 calAD	Oxcal v4.2 95.4%
T2S	149894	T2S-6	905	25	1038-1204 calAD	Oxcal v4.2 95.4%
T2S	149895	T2S-8	700	25	1264-1384 calAD	Oxcal v4.2 95.4%
T2S	149896	T2S-58	1125	25	779-990 calAD	Oxcal v4.2 95.4%
T2S	149905	T2S-50	1590	25	410-540 calAD	Oxcal v4.2 95.4%
T2S	149906	T2S-51	1000	25	987-1150 calAD	Oxcal v4.1.3 95.4%
T2S	149907	T2S-52	1000	25	987-1150 calAD	Oxcal v4.1.3 95.4%
T2S	149908	T2S-75	980	25	996-1154 calAD	Oxcal v4.2 95.4%
T2S	149909	T2S-76	1645	25	337-530 calAD	Oxcal v4.2 95.4%
T2S	149910	T2S-77	455	25	1417-1463 calAD	Oxcal v4.2 95.4%
T2S	149912	T2S-79	1505	25	433 - 622 calAD	Oxcal v4.2 95.4%
T2S	149913	T2S-80	2505	25	786 - 541 calBC	Oxcal v4.2 95.4%
T2S	149914	T2S-81	2045	30	165calBC-24calAD	Oxcal v4.2 95.4%
T2S	149915	T2S-3	750	25	1224-1285 calAD	Oxcal v4.2 95.4%
T2S	149916	T2S-4	1925	30	4 - 134 calAD	Oxcal v4.2 95.4%
T2S	PRI-10-130	BULK 1A	3295	20	1623 - 1518 calBC	Oxcal v4.2 95.4%
T2S	PRI-10-130	BULK 3A	1005	20	987 - 1118 calAD	Oxcal v4.2 95.4%
T2S	PRI-10-130	BULK 3B	890	20	1045 - 1214 calAD	Oxcal v4.2 95.4%
T2S	PRI-10-130	BULK 3C	1130	20	878 - 982 calAD	Oxcal v4.2 95.4%
T2S	PRI-10-130	BULK 3D	995	20	992 - 1148 calAD	Oxcal v4.2 95.4%
T2S	PRI-10-130	BULK 4A	955	20	1022 - 1155 calAD	Oxcal v4.2 95.4%
T2S	PRI-10-130	BULK 4B	1240	20	687 - 870 calAD	Oxcal v4.2 95.4%
T2S	PRI-10-130	BULK 4C	1000	20	988 - 1147 calAD	Oxcal v4.2 95.4%
T2S	PRI-10-130	BULK 4D	1115	20	890 - 982 calAD	Oxcal v4.2 95.4%
T3E	158554	CSS11 T3E C54	1035	25	970 - 1031 calAD	Oxcal v4.2 95.4%
T3E	158555	CSS11 T3E C63	1135	25	777 - 984 calAD	Oxcal v4.2 95.4%
T3E	158556	CSS11 T3E C66	935	25	1031 - 1157 calAD	Oxcal v4.2 95.4%
T3E	158773	CSS11 T3E C64	1135	30	777 - 986 calAD	Oxcal v4.2 95.4%
T3E	158469	CSS11 T3E C45	1025	25	974 - 1035 calAD	Oxcal v4.2 95.4%
T3E	158470	CSS11 T3E C44	850	25	1154 - 1258 calAD	Oxcal v4.2 95.4%
T3E	158471	CSS11 T3E C43	1275	25	673 - 771 calAD	Oxcal v4.2 95.4%
T3E	158472	CSS11 T3E C40	1735	25	244 - 381 calAD	Oxcal v4.2 95.4%
T3E	158473	CSS11 T3E C47	945	25	1027 - 1155 calAD	Oxcal v4.2 95.4%
T3E	PRI-12-063-B10	B10	4835	20	3658 - 3536 calBC	Oxcal v4.2 95.4%
T3E	PRI-13-103	11CSS-T3E-B1.A	865	22	1051 - 1225 calAD	Oxcal v4.2 95.4%
T3E	PRI-13-103	11CSS-T3E-B1.C	936	22	1032 - 1156 calAD	Oxcal v4.2 95.4%
T3E	PRI-13-103	11CSS-T3E-B1.B	1028	23	979 - 1030 calAD	Oxcal v4.2 95.4%
T3W	PRI-12-063-B9	B9	1540	15	428 - 570 calAD	Oxcal v4.2 95.4%
T3W		BULK 5A	940	20	1030 - 1155 calAD	Oxcal v4.2 95.4%
T3W		BULK 5C	1130	35	777 - 989 calAD	Oxcal v4.2 95.4%
T3W		BULK 6A	1000	20	988 - 1147 calAD	Oxcal v4.2 95.4%
T3W		BULK 6D	990	15	998 - 1147 calAD	Oxcal v4.2 95.4%
T3W		BULK 9	1540	15	428 - 570 calAD	Oxcal v4.2 95.4%
T4E	158557	CSS11 T4E C8	940	30	1025 - 1160 calAD	Oxcal v4.2 95.4%
T4E	158558	CSS11 T4E C30	950	30	1024 - 1155 calAD	Oxcal v4.2 95.4%
T4E	158559	CSS11 T4E C34	1025	35	901 - 1148 calAD	Oxcal v4.2 95.4%
T4E	158560	CSS11 T4E C36	1005	25	985 - 1148 calAD	Oxcal v4.2 95.4%
T4E	158561	CSS11 T4E C50	1260	35	668 - 868 calAD	Oxcal v4.2 95.4%
T4E	158625	CSS11 T4E C4	1190	25	769 - 938 calAD	Oxcal v4.2 95.4%
T4E	158626	CSS11 T4E C6	925	25	1032 - 1162 calAD	Oxcal v4.2 95.4%
T4E	PRI-12-063-BS4B	BS4	975	15	1018 - 1149 calAD	Oxcal v4.2 95.4%
T4E	PRI-12-063-BS10	BS10	1000	15	992 - 1040 calAD	Oxcal v4.2 95.4%
T4W	158562	CSS11 T4WC24	965	35	1015 - 1160 calAD	Oxcal v4.2 95.4%
T4W	158563	CSS11 T4W C37	940	25	1030 - 1155 calAD	Oxcal v4.2 95.4%
T4W	158566	CSS11 T4WC24 - dup	935	25	1031 - 1157 calAD	Oxcal v4.2 95.4%
T4W	158567	CSS11 T4W C37 - dup	975	25	1015 - 1155 calAD	Oxcal v4.2 95.4%
T4W	158474	CSS11 T4W C19	1000	35	976 - 1154 calAD	Oxcal v4.2 95.4%
T4W	158475	CSS11 T4W C20	985	25	994 - 1152 calAD	Oxcal v4.2 95.4%
T4W	158476	CSS11 T4W C21	>Modern		>Modern	Oxcal v4.2 95.4%
T4W	158477	CSS11 T4W C22	1380	25	614 - 674 calAD	Oxcal v4.2 95.4%
T4W	PRI-12-063-BS1	BS1	2975	15	1260 - 1127 calBC	Oxcal v4.2 95.4%
T4W	PRI-12-063-BS2A	BS2	975	20	1016 - 1152 calBC	Oxcal v4.2 95.4%
T4W	PRI-12-063-BS2B	BS2	1000	15	992 - 1040 calAD	Oxcal v4.2 95.4%
T5W	PRI-13-103	CSS-T5W-2012-BS-01.B	967	22	1018 - 1154 calAD	Oxcal v4.2 95.4%
T5W	PRI-13-103	CSS-T5W-2012-BS-01.A	1157	22	776 - 966 calAD	Oxcal v4.2 95.4%
T6S	PRI-13-103	CSS-T6S-12-BS1.B	601	23	1299 - 1406 calAD	Oxcal v4.2 95.4%
T6S	PRI-13-103	CSS-T6S-12-BS1.D	610	23	1297 - 1401 calAD	Oxcal v4.2 95.4%
T6S	PRI-13-103	CSS-T6S-12-BS1.C	627	23	1290 - 1397 calAD	Oxcal v4.2 95.4%
T6S	PRI-13-103	CSS-T6S-12-BS1.A	936	22	1032 - 1156 calAD	Oxcal v4.2 95.4%

RADIOCARBON DATING RESULTS

Crystal Springs South

AECOM

FUGRO

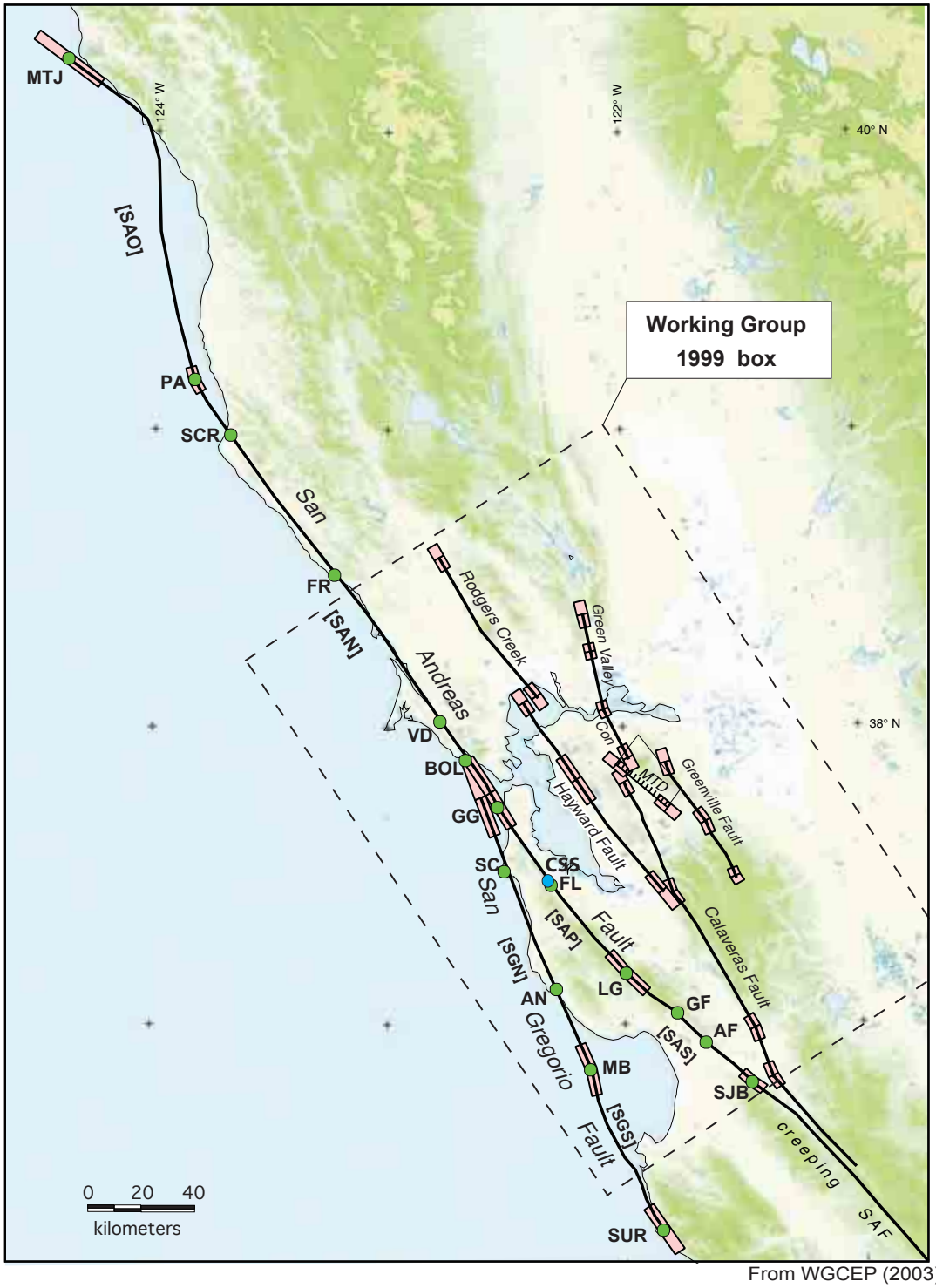

From WGCEP (2003)

Map of the northern San Andreas fault system, with segmentation (segment boundaries shown with pink boxes). From WGCEP (2003). Segments of San Andreas fault (SAF): SAO - Offshore; SAN - North Coast; SAP - Peninsula; SAS - Santa Cruz Mountains. Selected sites along SAF (dots): FL - Filoli; LG - Los Gatos bend in SAF; GF - Grizzly Flat; AR - Arano Flat; SJB - San Juan Bautista. Inset: WGCEP (2003) map of the Peninsula (SAP) and adjacent segments. CSS is Crystal Springs South site.

MAP OF THE NORTHERN SAN ANDREAS FAULT SYSTEM, INCLUDING THE PENINSULA SEGMENT (SAP)

Crystal Springs South

FIGURE 1

fwla-wc-file1/project/Projects/79_2000/79_223000_Crystal_Springs_South/05_Graphics

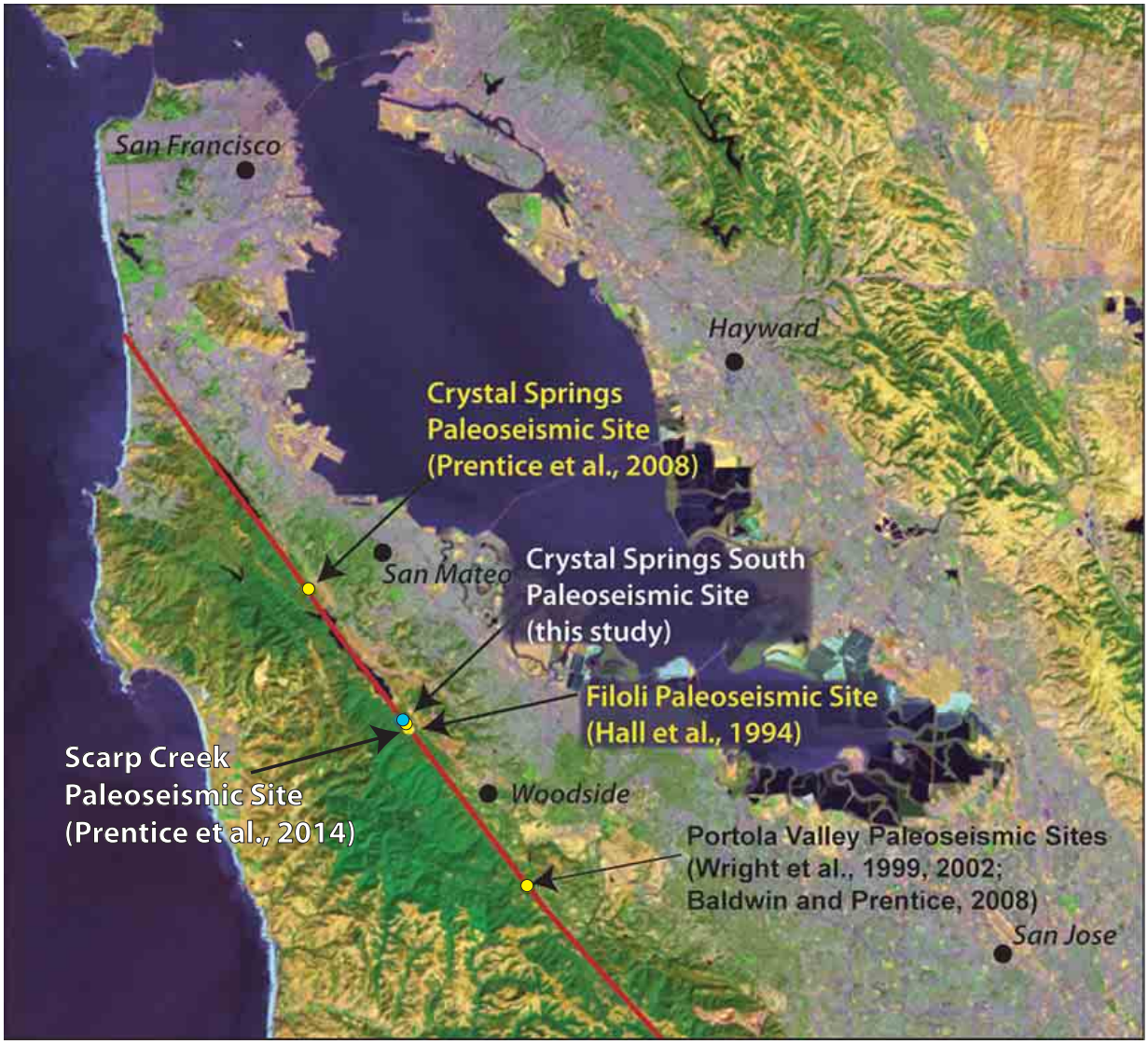

San Andreas fault Peninsula segment near Woodside, CA. Fault mapping from USGS Quaternary fault and fold database (http://earthquake.usgs.gov/regional/qfaults/). Colored dots show existing paleoseismic sites, including this study (blue dot).

fwla-wc-file1/project/Projects/79_2000/79_223000_Crystal_Springs_South/05_Graphics

SAN ANDREAS FAULT PENINSULA SEGMENT NEAR WOODSIDE, CA

Crystal Springs South

FIGURE 2

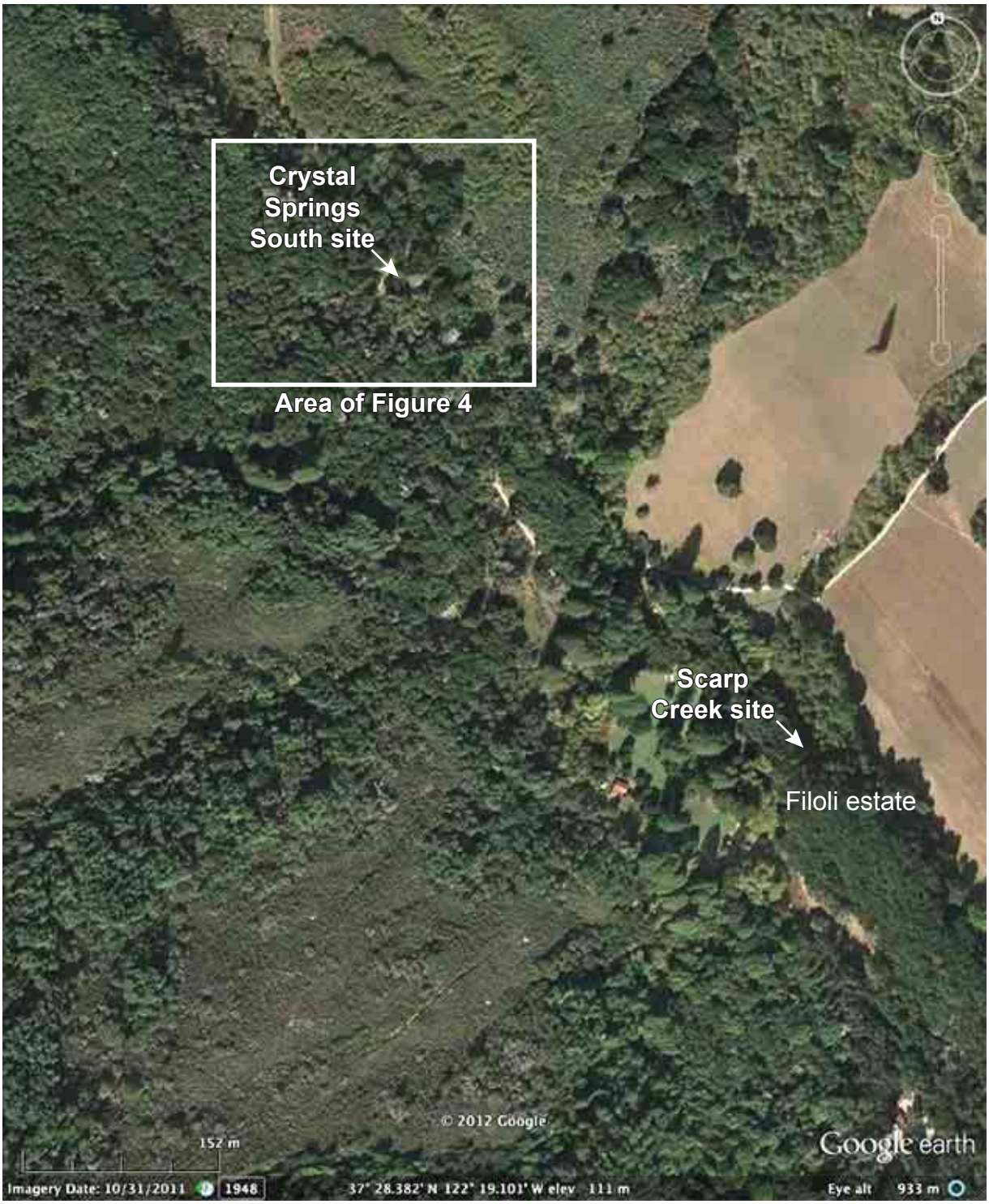

San Andreas fault is obscured by heavy vegetation.

AERIAL PHOTOGRAPH FROM GOOGLE EARTH SHOWING REGION BETWEEN SOUTHERN END OF CRYSTAL SPRINGS RESERVOIR AND FILOLI ESTATE

Crystal Springs South

FIGURE 3

fwla-wc-file1/project/Projects/79_2000/79_223000_Crystal_Springs_South/05_Graphics

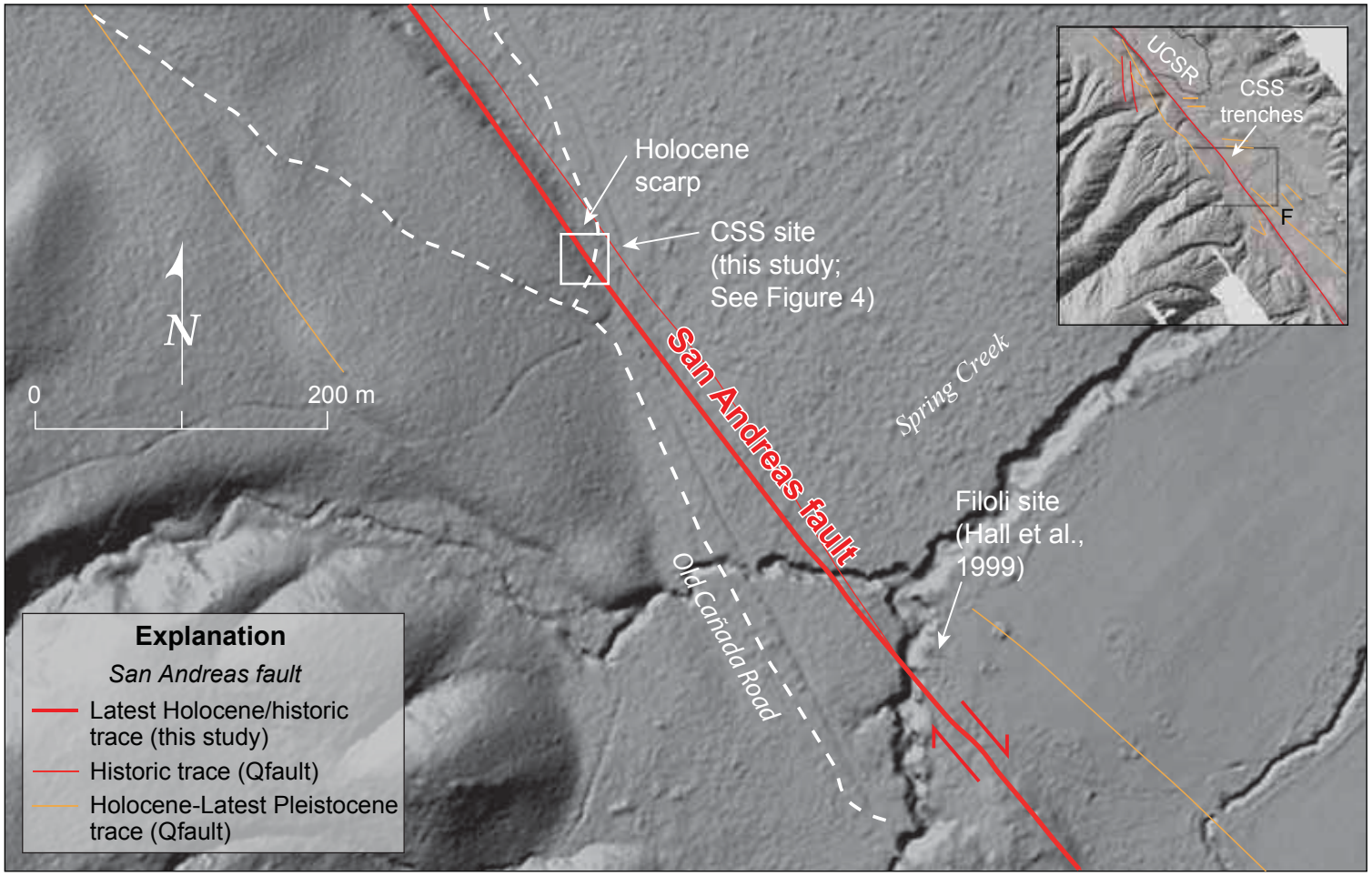

Bare earth DEM obtained from National Science Foundation Geoearthscope LiDAR data of Crystal Springs South (CSS) site. Faults in light line weight are from USGS Quaternary fault database ("Qfault") map (USGS/CGS, 2006; compiled at 1:750,000). Modified fault mapping between CSS site and Filoli site (done for this study) is shown in heavy line weight. Trenches excavated in 2010 shown on Figure 4 cross the fault where a small latest Holocene scarp is present outboard of the higher, eroded scarp. CSS trench site is protected from high stream flows by the fault scarp, which is eroded back from the fault and buried by fan deposits. Inset shows location of site relative to Upper Crystal Springs reservoir (UCSR) and Filoli Estates (F); faults from USGS/CGS (2006).

SITE MAP WITH BARE EARTH DEM OBTAINED FROM LIDAR DATA OF CRYSTAL SPRINGS SOUTH SITE

Crystal Springs South

FIGURE 4

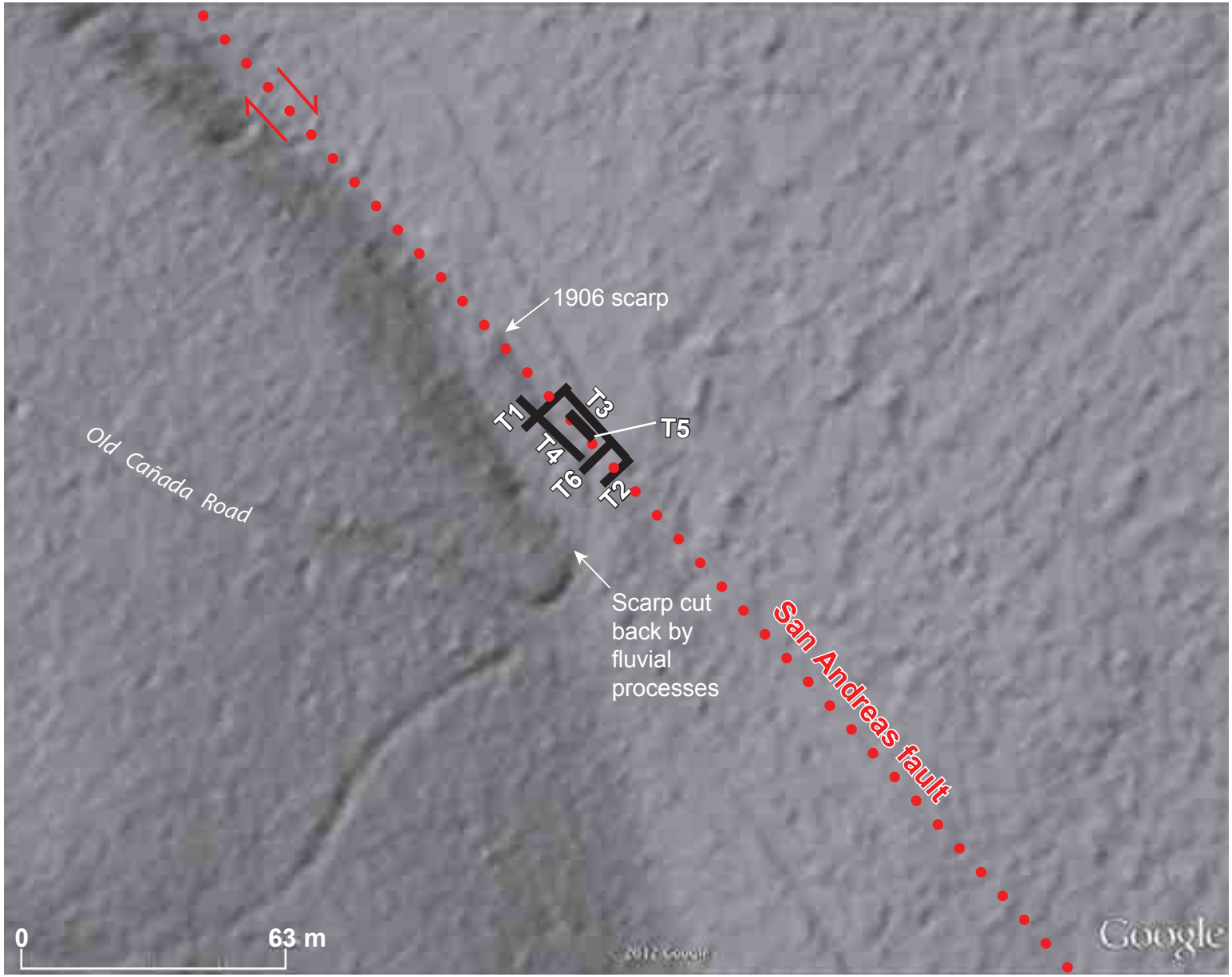

Hillshade image from LiDAR data showing blow-up of CSS trench site and six trench locations. Red dots mark active trace of San Andreas Fault. Three trenches (T1, T2, T6) cross the fault zone; T3, T4, and T5 are parallel to the fault. T1 crosses subtle scarp marking 1906 fault trace. Area is underlain by recent fluvial deposits related to Spring Creek. Southeast of trench site young surface shows little to no expression of active fault trace.

MAP OF TRENCH SITE LOCATIONS

Crystal Springs South

FIGURE 5

Crystal Springs South Paleoseismic Investigation

AECOM

FUGRO

Photograph of trench site. View is to the south. Red line marks approximate location of fault.

PHOTOGRAPH OF TRENCHES T1 AND T2

Crystal Springs South

FIGURE 6

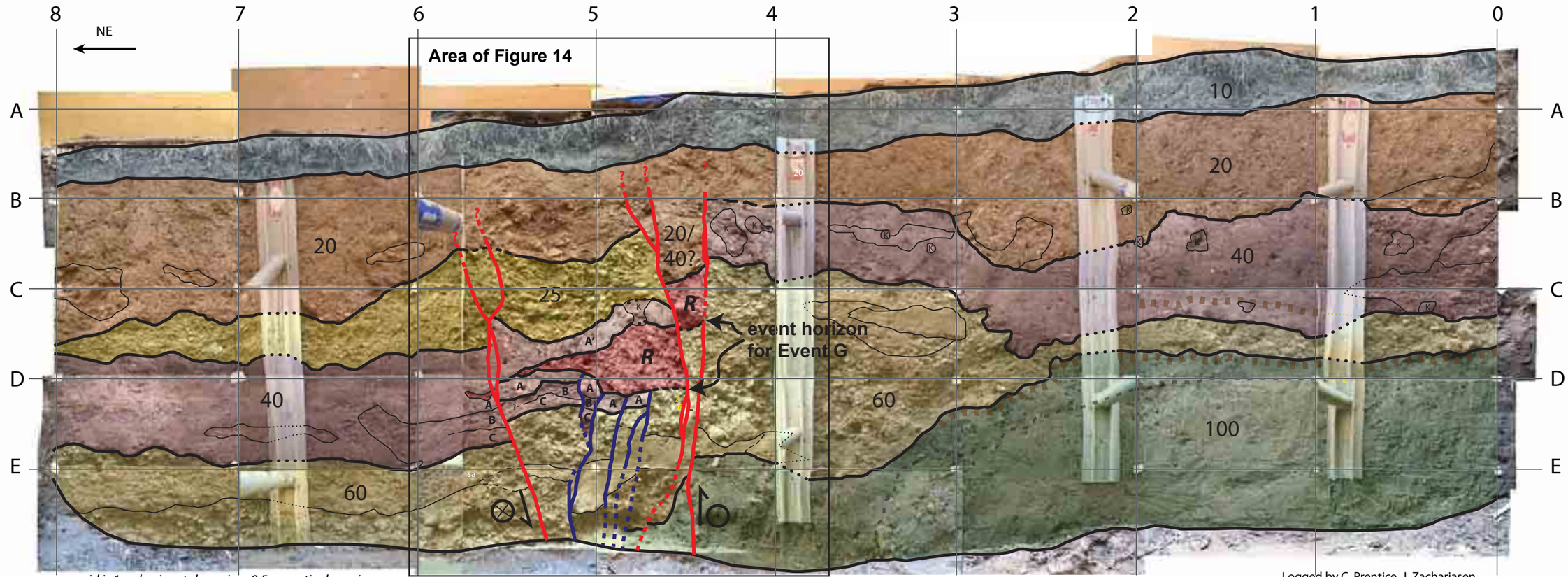

Explanation

10	Topsoil (A horizon)
20	Massive sandy pebbly silt with abundant bioturbation
25	Well-rounded pebble-cobble gravel in coarse sand matrix; present only on downthrown side
R	Colluvial wedge rubble, derived from unit 60; chaotic pebble-cobble gravel
40	Brown, massive, silty fine sand to sandy silt, with scattered pebbles and abundant charcoal; hatchures mark paleosol. Fault zone sub-units: A (pre-Event G) - silty sand; A' (Post-Event G) - very fine sandy silt; B - sandy granule gravel; C- sand
60	Channel complex; well-rounded, clast-supported pebble-cobble gravel, with lenses of finer sand and silt
100	Grey, mottled sandy silty clay to clayey silty sand with scattered pebbles and sparse large clasts; clasts deeply weathered; hatchures mark change in color form dark grey above to orange mottled below

"K" indicates krotovina
Light line weight contacts mark lenses of different material within numbered unit

Most recent event (1906?) fault traces

Penultimate event ("event G") fault traces

Color change in unit 100: medium grey above, light grey with orange mottling below

Paleosol

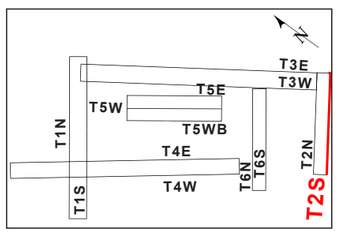

Location of Figure

Log of southeast wall of Trench T2. Trench exposed late Holocene coarse-grained channel and fine -grained overbank material interbedded with scarp-derived colluvium. Units in Trench T1 do not necessarily correlate with units with same numbers in Trench T2. Stratigraphic and structural relations provide evidence for two ground rupturing events : (1) the MRE (presumably 1906) is expressed by fault strands (shown in red) approaching the ground surface and terminating in a heavily bioturbated zone that is overlain by recent sediment; (2) The penultimate event (Event G) represents the displacement of the lower part of unit 40 (sub-unit "A" constituted the ground surface in Event G) across several fault strands (shown in purple). Event G exposed units 40 and 60, generating cobbly colluvium (R) derived from unit 60 that was deposited onto the paleo-surface "A". Deposition of unit 40 (A') overbank silts continued after Event G. Radiocarbon analysis of detrital charcoal from pre- and post-event deposits (A and A', respectively) indicate that Event G occurred about 600-1000 years ago.

LOG OF SOUTHEAST WALL OF TRENCH T2
Crystal Springs South

FIGURE 7A

fwla-wc-file1/project/Projects/79_2000/79_223000_Crystal_Springs_South/05_Graphics

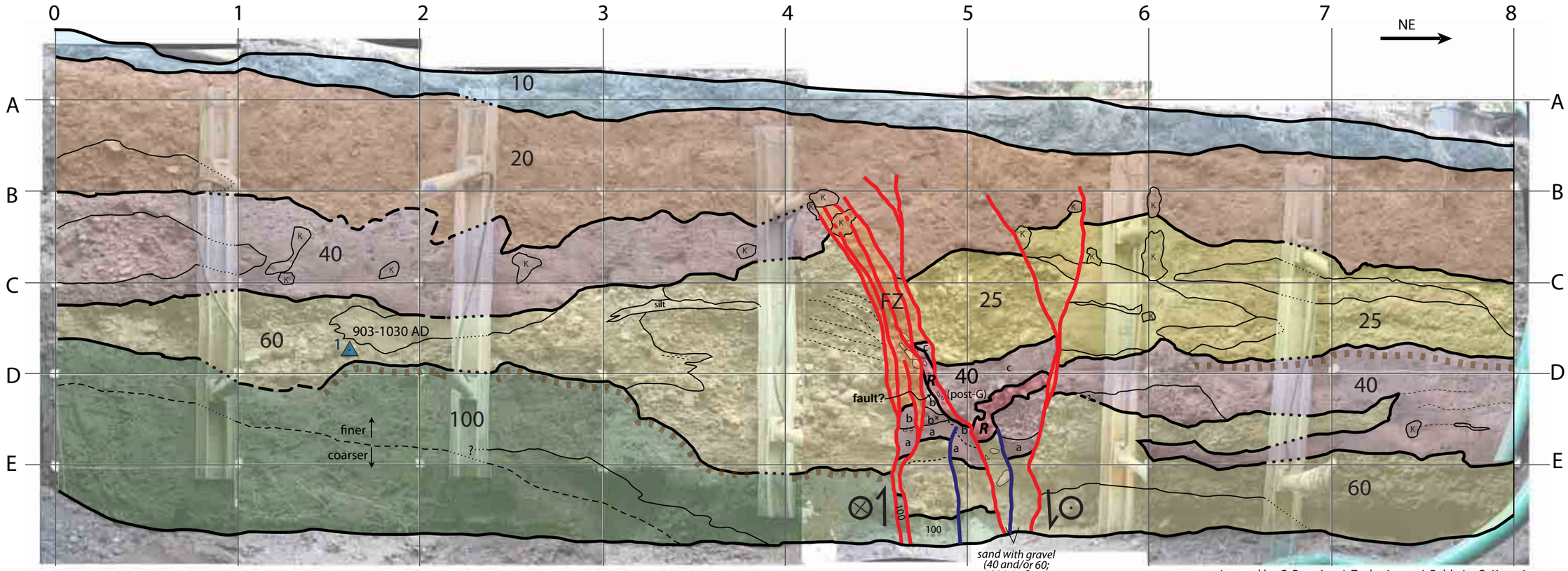

grid is 1-m horizontal spacing, 0.5-m vertical spacing

Logged by C. Prentice, J. Zachariasen, J. Baldwin, O. Kozaci
August 2010

Explanation

10	Topsoil (A horizon)
20	Massive sandy pebbly silt with abundant bioturbation
25	Well-rounded pebble-cobble gravel in coarse sand matrix; present only on downthrown side
40	Brown, massive, silty fine sand to sandy silt, with scattered pebbles and abundant charcoal; hatchures mark paleosol. Fault zone sub-units: a) clean sand within channel complex; b) silty sand with pebbles (b* more gravel, pebble gravel in m-f sandy matrix), pre-G; c) post-event G sandy silt
R	Colluvial wedge rubble, derived from unit 60; chaotic pebble-cobble gravel; in westernmost sliver of R, f-c pebble gravel is mostly f-c pebbles in a silty matrix (possibly including 40c, post-G silt), sheared in 1906 fault zone
FZ	Sheared gravel, silt and sand in fault zone
60	Channel complex; well-rounded, clast-supported pebble-cobble gravel, with lenses of finer sand and silt
100	Grey, mottled sandy silty clay to clayey silty sand with scattered pebbles and sparse large clasts; clasts deeply weathered; hatchures mark change in color form dark grey above to orange mottled below

903-1030 AD 1 — Radiocarbon sample location with calibrated age.

Most recent event (1906?) fault traces

Penultimate event ("event G") fault traces

Bedding

Paleosol

"K" indicates krotovina
Light line weight contacts mark lenses of different material within numbered unit

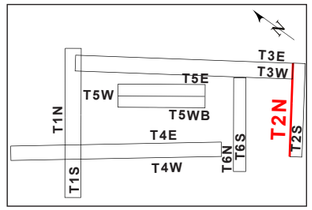

Location of Figure

LOG OF NORTHWEST WALL OF TRENCH T2
Crystal Springs South

FIGURE 7B

wla-wc-PROJECT/Projects/Project Number Project Name/05_Graphics, modified date

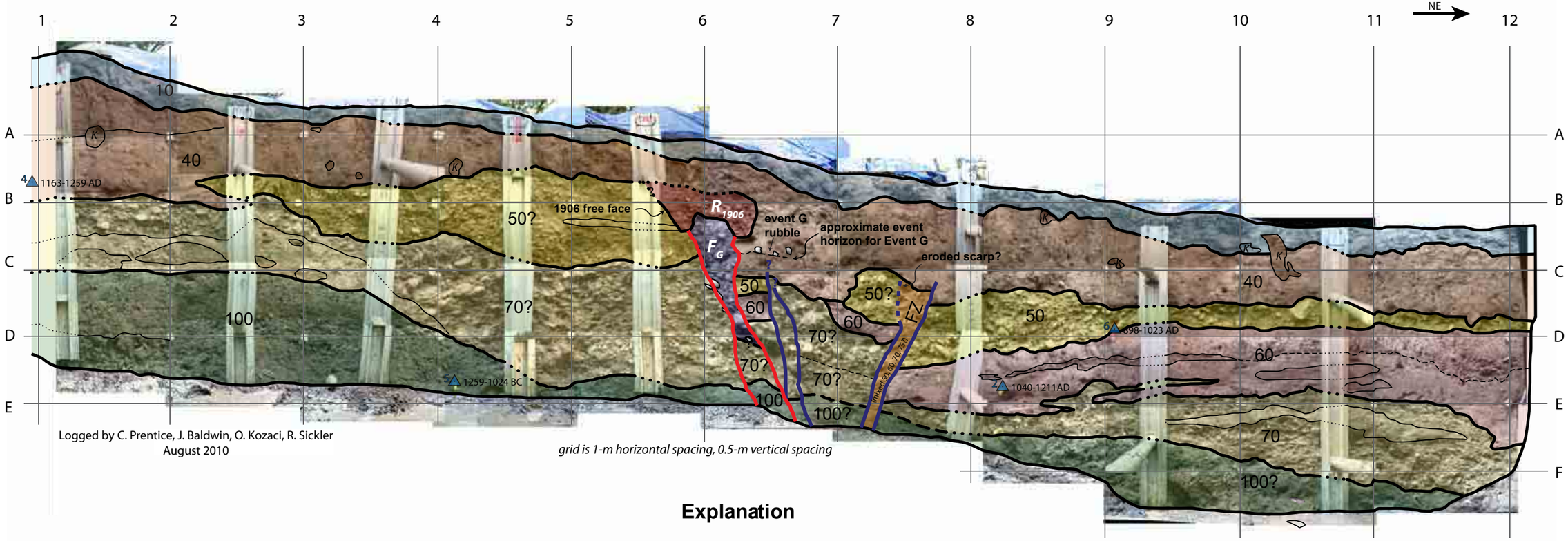

Logged by C. Prentice, J. Baldwin, O. Kozaci, R. Sickler
August 2010

grid is 1-m horizontal spacing, 0.5-m vertical spacing

Explanation

10	Topsoil (A horizon)
40	Massive pebbly sandy silt with abundant bioturbation
R_{1906}	Post-1906 colluvium; loose cobble gravel with coarse sand and small pebble matrix
F_G	Fissure fill, formed in Event G; faulted in 1906; chaotic pebble-cobble gravel
FZ	Sheared gravel, silt and sand in fault zone
50	Channel complex; loose, poorly sorted, mstrix-supported, pebble gravel in coarse sand matrix; massive to crudely bedded
60	Brown, massive, andy silt, with scattered pebbles and abundant charcoal
70	Channel complex; loose, poorly sorted, massive, matrix- to clast-supported, cobble gravel in coarse sand-pebble matrix
100	Grey, mottled sandy silty clay to clayey silty sand with scattered pebbles and sparse large clasts; clasts deeply weathered; hatchures mark change in color form dark grey above to orange mottled below
4 1163-1259 AD	Radiocarbon sample location with calibrated age.
	Most recent event (1906?) fault traces
	Penultimate event ("event G") fault traces

"K" indicates krotovina
Light line weight contacts mark lenses of different material within numbered unit

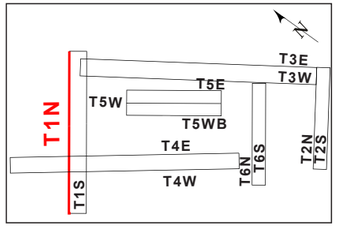

Location of Figure

Log of northwest wall of Trench T1. Late Holocene coarse-grained channel and fine-grained overbank deposits are displaced by multiple near-vertical to steeply dipping fault strands. Stratigraphic and structural relations provide evidence for two ground rupturing events: (1) the MRE (presumably 1906) is expressed by fault strands (shown in red) approaching the ground surface and terminating in a heavily bioturbated zone. The fault terminations are overlain by a colluvial wedge (R1906) composed of gravelly rubble raveled off the 1906 scarp face; (2) The penultimate event (Event G) represents the displacement of the lower part of unit 40 across several fault strands (shown in purple). Event G exposed units 50, 60 and 70, generating cobbly colluvium that appears as a few scattered cobbles within the lower part of unit 40. Event G also produced a fissure (FG), which was subsequently faulted in 1906. Deposition of unit 40 overbank silts continued after Event G.

LOG OF NORTHWEST WALL OF TRENCH T1

FIGURE 8

wla-wc-PROJECT/Projects/Project Number Project Name/05_Graphics, modified date

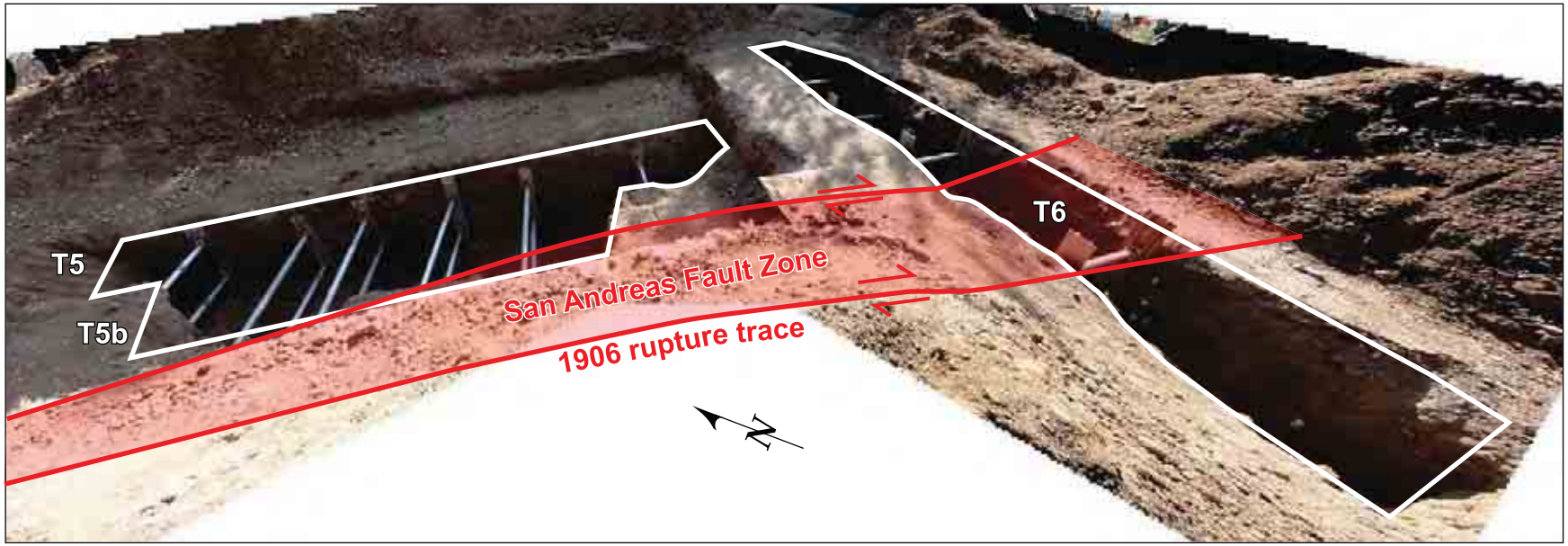

PHOTOGRAPH OF TRENCHES T5 AND T6
Crystal Springs South

FIGURE 9

AECOM

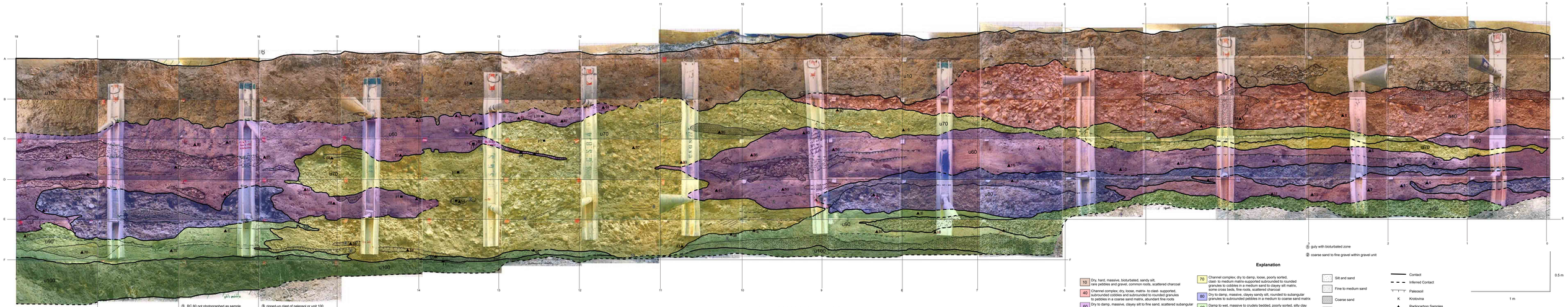

① RC 60 not photographed as sample
② RC 67 don't use, Krotovina
③ ripped-up clast of paleosol or unit 100
④ dark pebbly silty sand

① this area is very distorted, contact is not this steep
② fine sand lens
③ silty clay; grey
④ cross beds of coarse sand and pebbly gravel
⑤ silty very fine to fine sand; abundant charcoal; overall darkened unit represents period of stability within BFC; separates upper, youngest phase of BFC from lower, older phases.
⑥ silty very fine sand with no obvious bioturbation
⑦ upper part of gravel is bioturbated
⑧ 4 cm bed of clast supported well rounded pebbles
⑨ medium to coarse sand planer beds
⑩ gravel to water level

T3, East

① upper part of gravel is bioturbated
② move shore, BFC pinch or continue?
③ base of paleosol
④ silty very fine sand with organics, poorly defined paleosol
⑤ fine sand
⑥ slightly dark silty very fine sand, scoured by overlying BFC

① guly with bioturbated zone
② coarse sand to fine gravel within gravel unit

Explanation

10	Dry, hard, massive, bioturbated, sandy silt, rare pebbles and gravel, common roots, scattered charcoal
40	Channel complex; dry, loose, matrix- to clast- supported, subrounded cobbles and subrounded to rounded granules to pebbles in a coarse sand matrix, abundant fine roots
60	Dry to damp, massive, clayey silt to fine sand, scattered subangular cobbles and pebbles, some coarse sand and gravel lenses, abundant fine to medium roots, scattered charcoal
70	Channel complex; dry to damp, loose, poorly sorted, clast- to medium matrix-supported subrounded to rounded granules to cobbles in a medium sand to clayey silt matrix, some cross beds, fine roots, scattered charcoal
80	Dry to damp, massive, clayey sandy silt, rounded to subangular granules to subrounded pebbles in a medium to coarse sand matrix
90	Damp to wet, massive to crudely bedded, poorly sorted, silty clay to sandy silt, medium to coarse sand, granules to subangular pebbles, rare roots, abundant charcoal
100	Wet, massive, silty clay to clay, scattered fine to coarse sand, rare roots

Silt and sand
Fine to medium sand
Coarse sand
Sand and pebbles
Sand and pebble to cobbles

Contact
Inferred Contact
Paleosol
K Krotovina
Radiocarbon Samples
Pollen Samples
Bulk Samples

0.5 m
1 m

Location of Figure

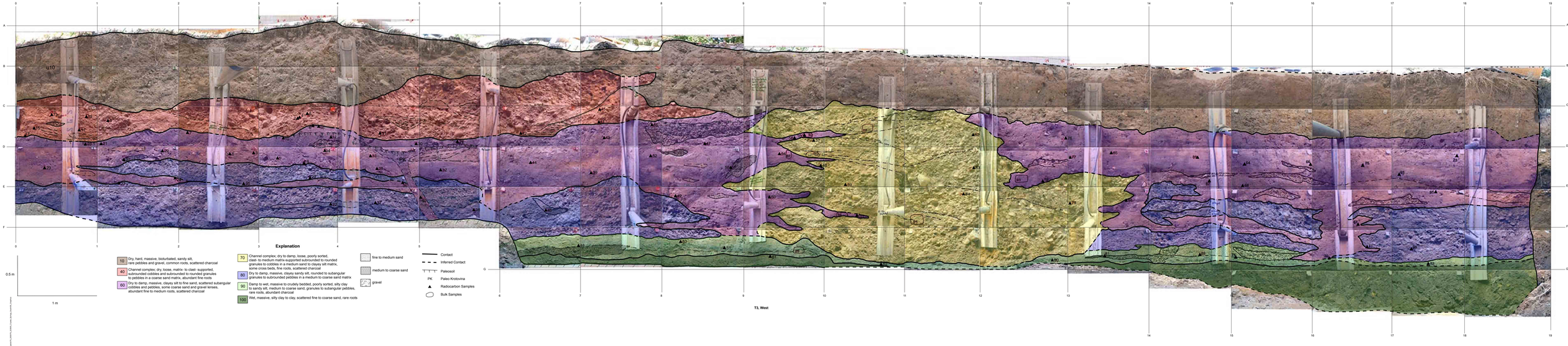

Explanation

10	Dry, hard, massive, bioturbated, sandy silt, rare pebbles and gravel, common roots, scattered charcoal
40	Channel complex; dry, loose, matrix- to clast- supported, subrounded cobbles and subrounded to rounded granules to pebbles in a coarse sand matrix, abundant fine roots
60	Dry to damp, massive, clayey silt to fine sand, scattered subangular cobbles and pebbles, some coarse sand and gravel lenses, abundant fine to medium roots, scattered charcoal
70	Channel complex; dry to damp, loose, poorly sorted, clast- to medium matrix-supported subrounded to rounded granules to cobbles in a medium sand to clayey silt matrix, some cross beds, fine roots, scattered charcoal
80	Dry to damp, massive, clayey sandy silt, rounded to subangular granules to subrounded pebbles in a medium to coarse sand matrix
90	Damp to wet, massive to crudely bedded, poorly sorted, silty clay to sandy silt, medium to coarse sand, granules to subangular pebbles, rare roots, abundant charcoal
100	Wet, massive, silty clay to clay, scattered fine to coarse sand, rare roots

fine to medium sand
medium to coarse sand
gravel

Contact
Inferred Contact
Paleosol
PK Paleo Krotovina
Radiocarbon Samples
Bulk Samples

0.5 m
1 m

T3, West

TRENCH T3, EAST AND WEST
Crystal Springs Reservoir

FIGURE 10

Y:\01-Projects\Projects\CSPR\CSPR\Trench\Trench T3 East and West.dwg

AECOM

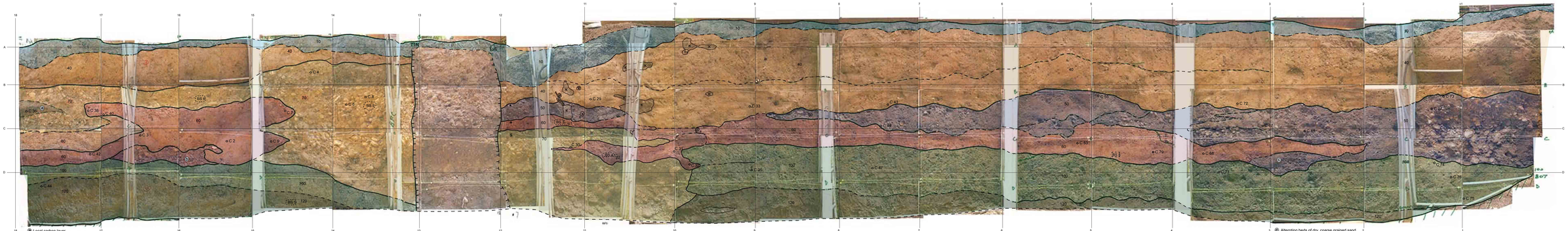

Trench T4, East

Explanation

- 10 Topsoil
- 40 Massive, fine grained clayey sand, scattered subrounded to well rounded pebbles, abundant roots, bioturbation, scattered charcoal, few crotovina
- 50 Channel deposits- dry, loose, coarse sand matrix, coarsely bedded, subrounded pebbles to subrounded and subangular cobbles, scattered fine roots, rare charcoal
- 60 Massive, damp, clayey silt, rare subrounded pebbles, common lenses of alternating pebbled beds and charcoal
- 70 Channel complex- Medium to coarse sand matrix including subrounded pebbles to cobbles, fine roots, scattered charcoal, crudely bedded, few organic lenses
- 80 Dry, coarse sand matrix, subrounded pebbles, clast supported (at base) to crudely bedded coarse sand matrix (at top)
- 100 Massive, damp to we clayey silt, scattered subrounded pebbles, rare roots
- 120 Massive, wet, silty clay
- Trench fill material from T1

Units correlate on T1S column 4-5

"K" indicates krotovina

"Rx" indicates rock

"P" indicates pebble

Carbon Sample

Bulk Sample

Pollen Sample

Location of Figure

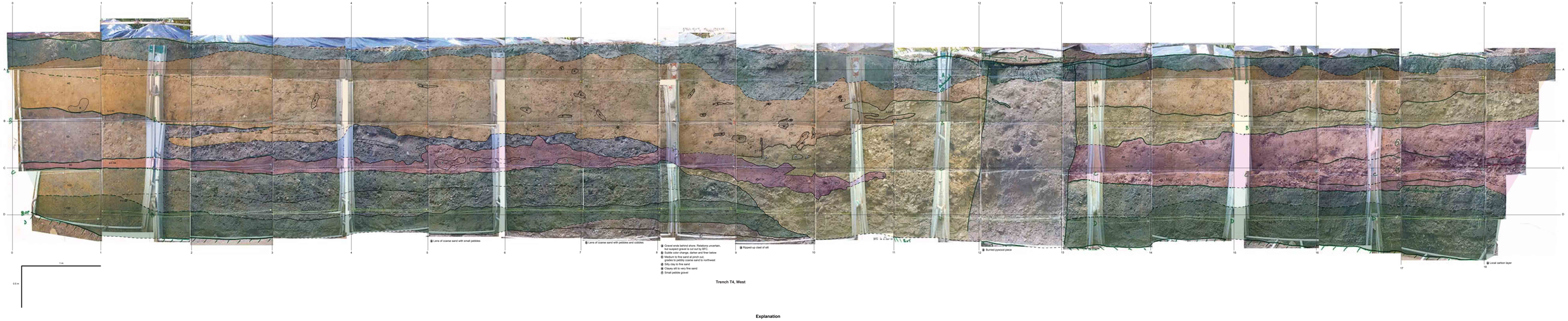

Trench T4, West

Explanation

- 10 Topsoil
- 40 Massive, fine grained clayey sand, scattered subrounded to well rounded pebbles, abundant roots, bioturbation, scattered charcoal, few crotovina
- 50 Channel deposits- dry, loose, coarse sand matrix, coarsely bedded, subrounded pebbles to subrounded and subangular cobbles, scattered fine roots, rare charcoal
- 60 Massive, damp, clayey silt, rare subrounded pebbles, common lenses of alternating pebbled beds and charcoal
- 70 Channel complex- Medium to coarse sand matrix including subrounded pebbles to cobbles, fine roots, scattered charcoal, crudely bedded, few organic lenses
- 100 Massive, damp to we clayey silt, scattered subrounded pebbles, rare roots
- 120 Massive, wet, silty clay
- Trench fill material from T1

"K" indicates krotovina

"r" indicates root

Carbon Sample

Bulk Sample

Pollen Sample

Source: Aerial photo from Google Earth, 2/28/2011, Contour Interval 2 feet

TRENCH T4, EAST AND WEST
Crystal Springs Reservoir

FIGURE 11

AECOM

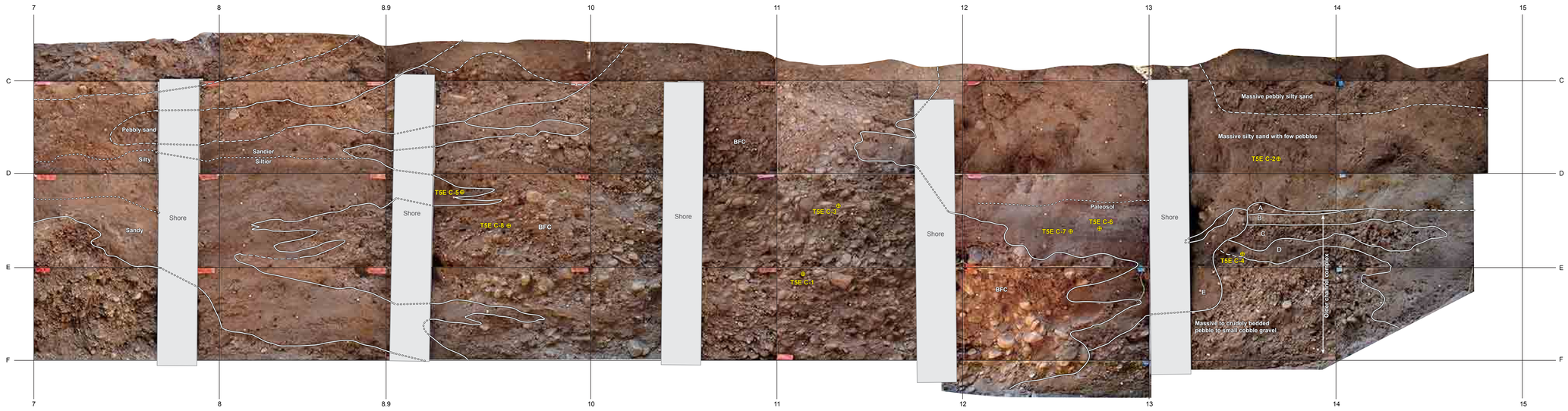

Trench T-5, East

Explanation

- Contact, dashed where uncertain
- Contact, concealed
- Subunit contact
- Pebble lines
- BS2 — Bulk sample
- T5Sb C-2 — Radiocarbon sample

Subunits of older channel complex

- A Small pebbles in sandy silt matrix
- B Silty fine sand with few pebbles
- C Small pebble gravel and coarse sand interbeds
- D Silty fine sand
- E Massive fine to very fine sand with few pebbles; steep erosional contact

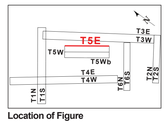

Location of Figure

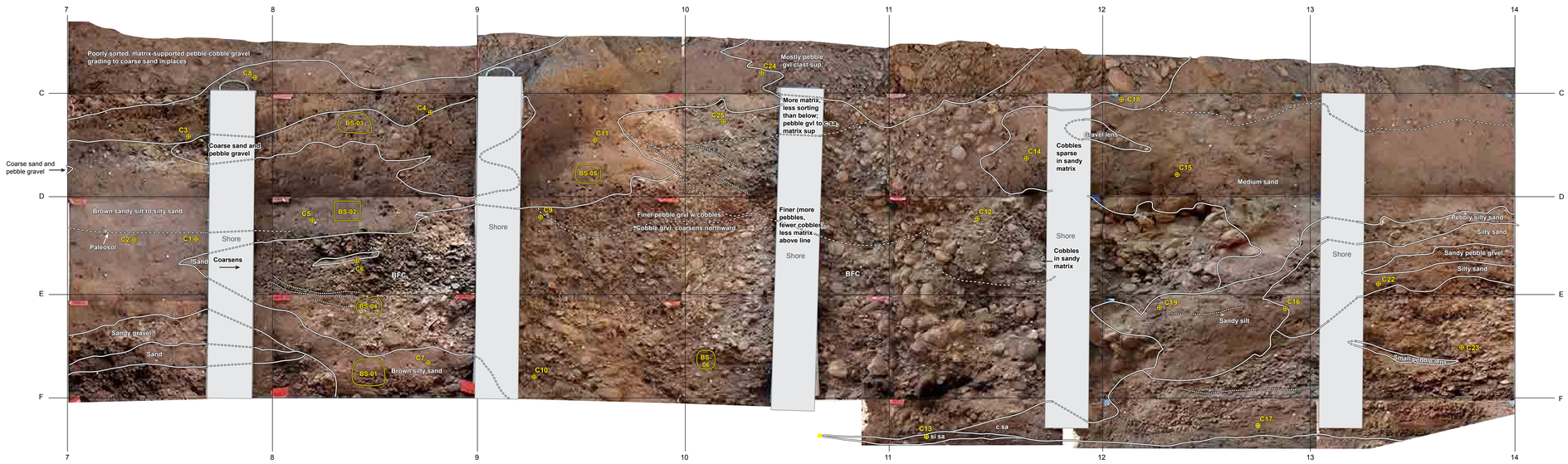

Trench T-5, West

Explanation

- Contact
- Contact, concealed
- Subunit contact, queried where uncertain
- Pebble lines
- BS2 — Bulk sample
- T5Sb C-2 — Radiocarbon sample
- ? Fault; dashed and queried where uncertain
- Krotovina

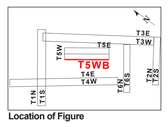

Location of Figure

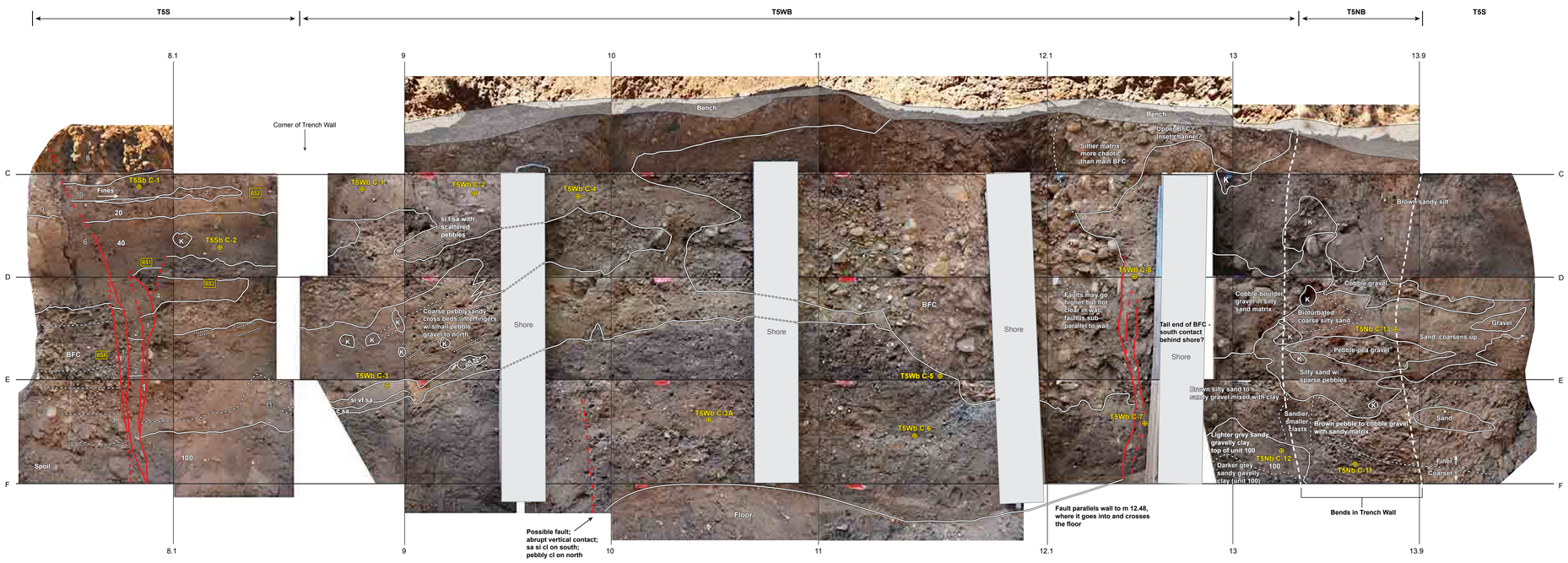

Trench T-5, West, B

Explanation

- Contact
- Contact, concealed
- Subunit contact
- Pebble lines
- BS2 — Bulk sample
- T5Sb C-2 — Radiocarbon sample

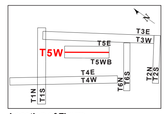

Location of Figure

Trench T5W, T5WB, and T5E
Cyrstal Springs Reservoir

FIGURE 12

79_223000 Crystal Springs Trench Logs_082714 at Wednesday, August 27 2014 08:28:02

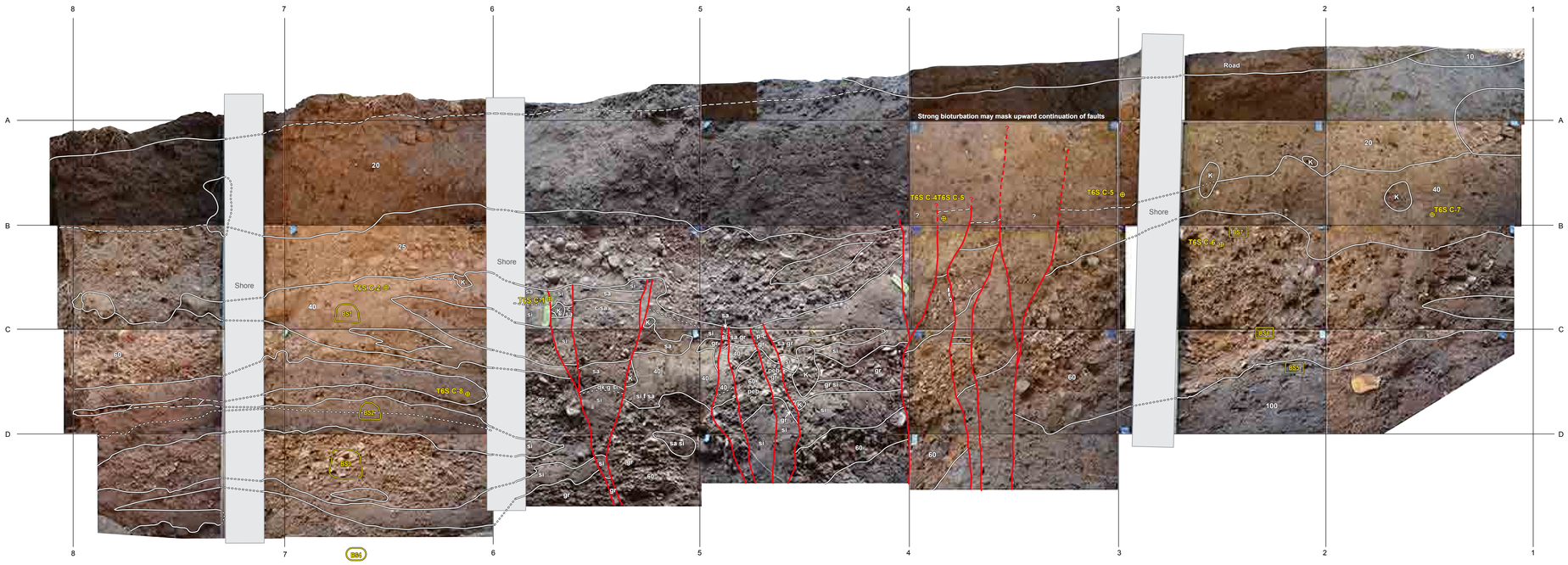

Contact
Contact, concealed
Subunit contact
Pebble lines
Contact, uncertain
Paleosol
BS2 Bulk sample
T5Sb C-2 Radiocarbon sample
Fault; dashed and queried where uncertain

Abbreviations
c Coarse
sa Sand
si Silt
dk Dark
g Gray
f Fine
peb Pebbles
gr Gravels
p Partially
K Krotovina

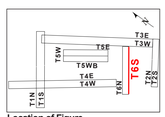

Location of Figure

Trench T-6, South

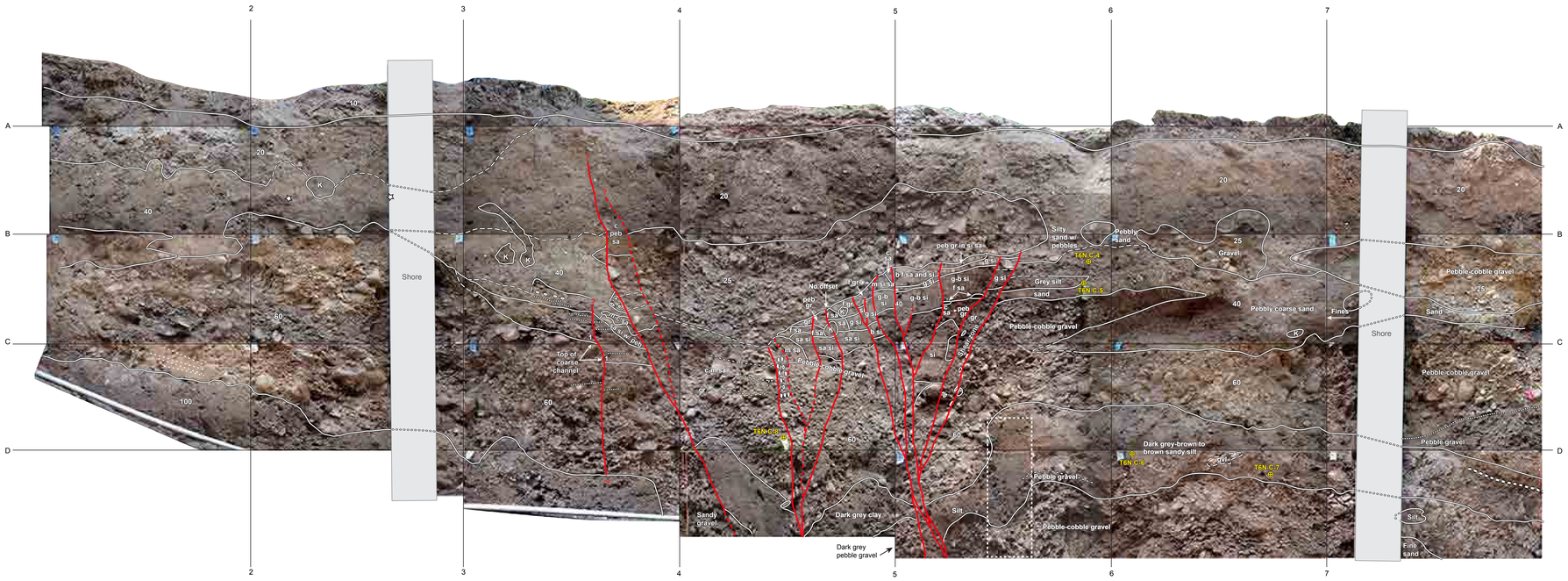

Contact
Contact, concealed
Subunit contact
Pebble lines
Contact, uncertain
Paleosol
BS2 Bulk sample
T5Sb C-2 Radiocarbon sample
Define
Fault; dashed and queried where uncertain

Abbreviations
c Coarse
sa Sand
si Silt
dk Dark
g Gray
f Fine
peb Pebbles
gr Gravels
p Partially
m Medium
K Krotovina

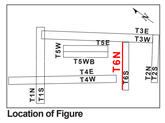

Location of Figure

Trench T-6, North

Trench T6, North and South
Cyrstal Springs Reservoir

FIGURE 13

79_223000 Crystal Springs Trench Logs_GEOT14.ai Wednesday, August 27 2014 08:27:45

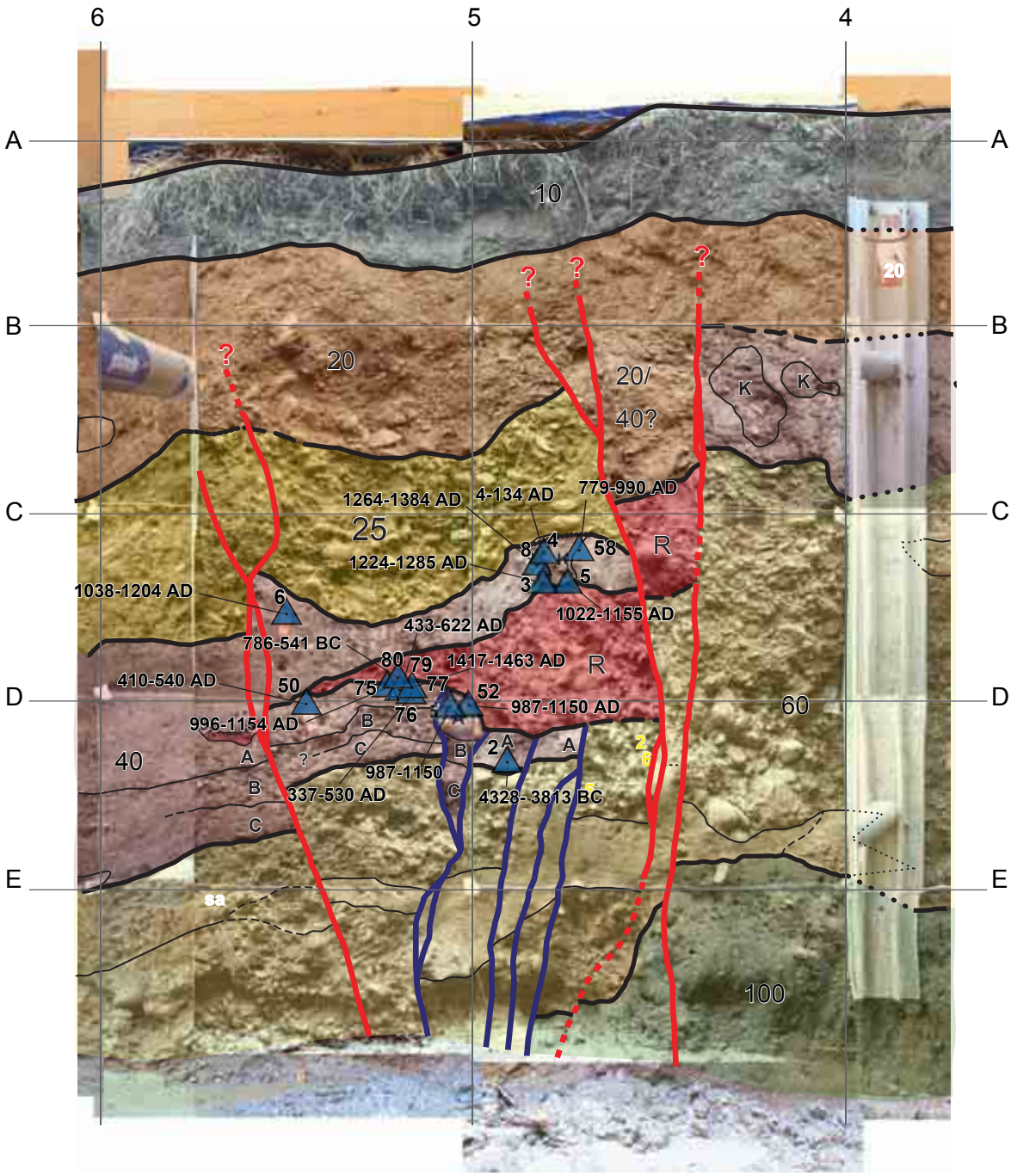

Close-up of the fault zone in the southeastern wall of Trench T2. Several charcoal samples from the overbank silts (unit 40) that pre-date and post-date the colluvial wedge "R" formed after Event G were dated to provide constraints on the age of the event. Sample locations are marked with blue triangles, with sample number and calibrated date range indicated. Results are tabulated in Table 1. See Figure 7a for explanation of units.

fwla-wc-file1/project/Projects/79_2000/79_223000_Crystal_Springs_South/05_Graphics

CLOSE-UP OF THE FAULT ZONE IN THE SOUTHERN WALL OF TRENCH T2 WITH RADIOCARBON SAMPLES

Crystal Springs South

FIGURE 14

Event G

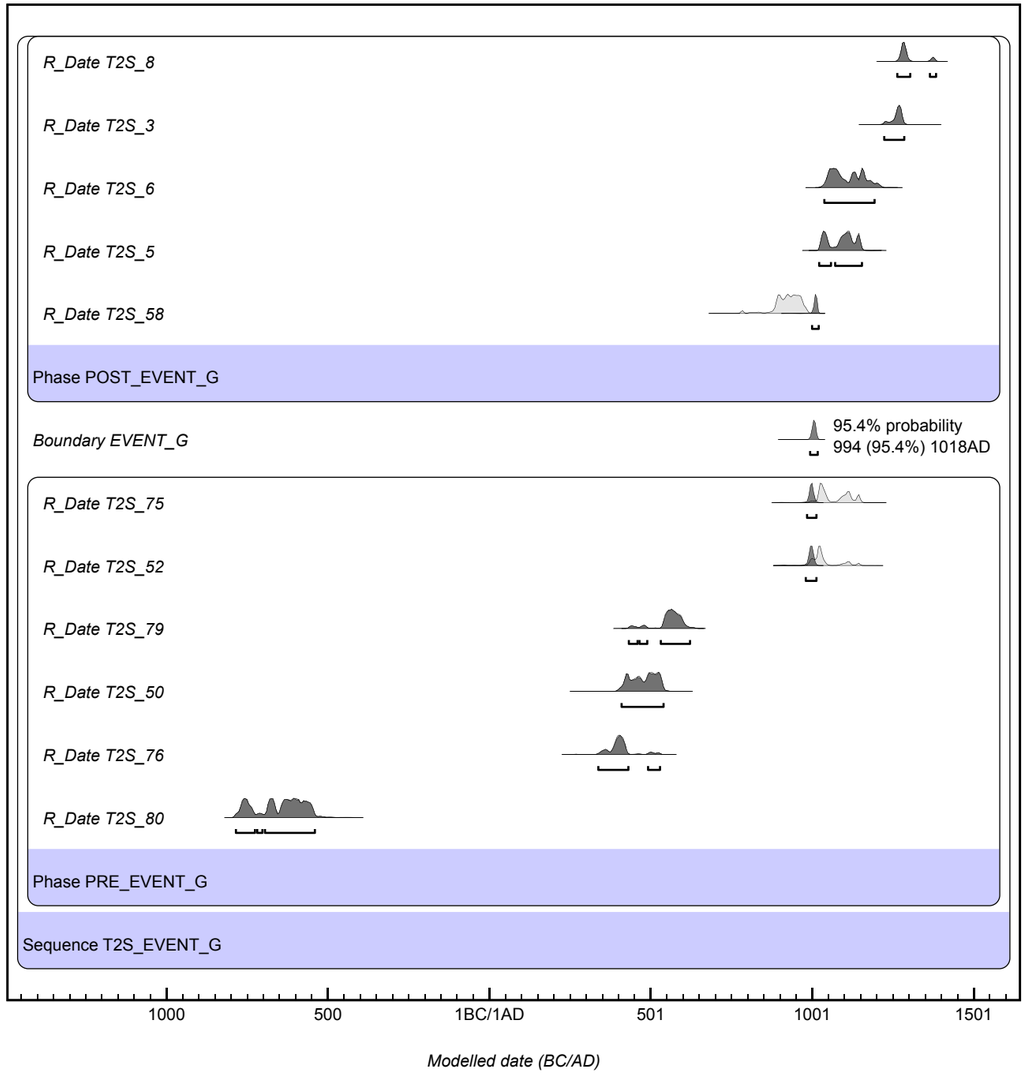

Offset Channel

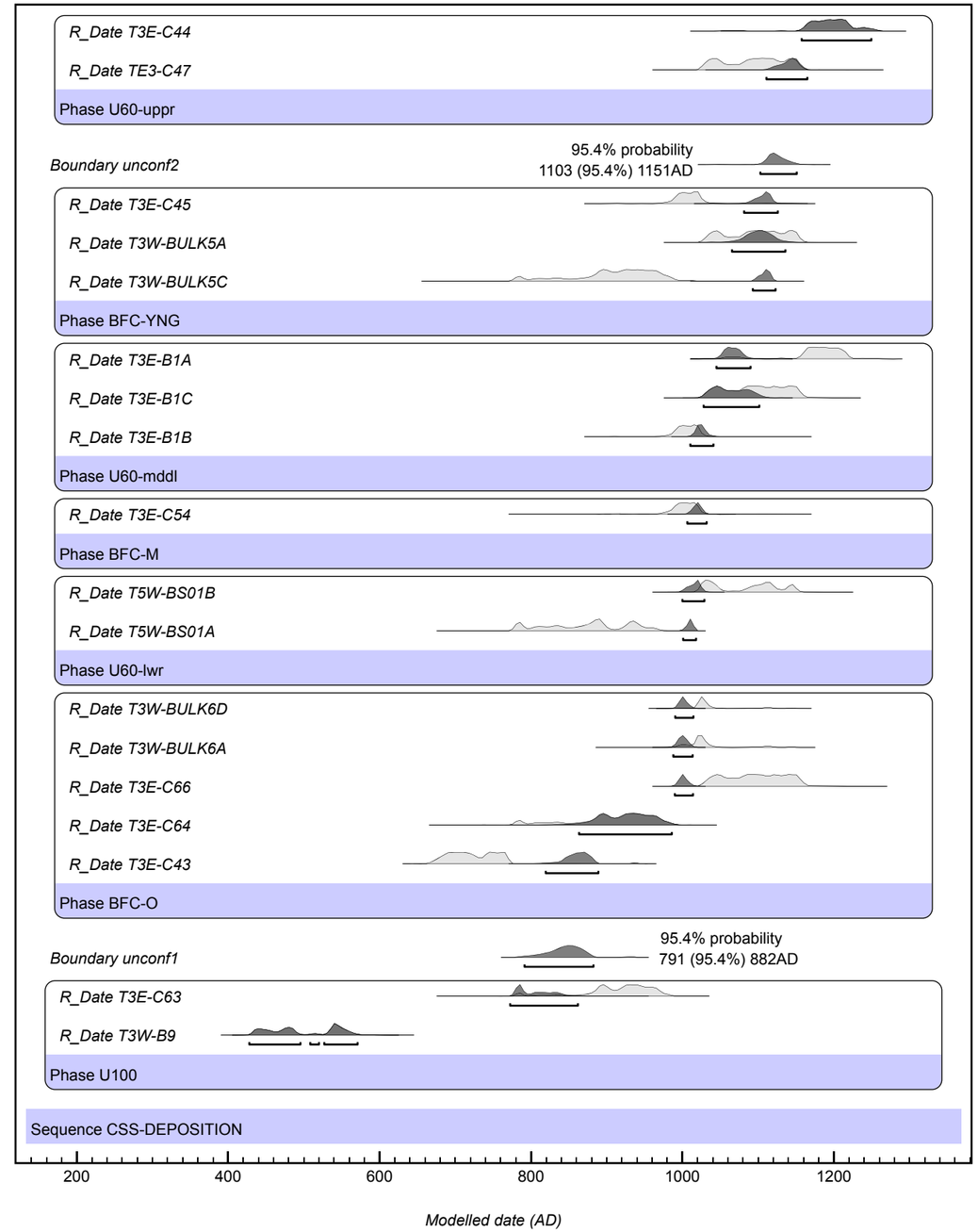

OxCal v4.2.4 Bronk Ramsey (2013); r:5 IntCal13 atmospheric curve (Reimer et al 2013)

fwla-wc-file1/project/Projects/79_2000/79_223000_Crystal_Springs_South/05_Graphics

OXCAL MODELS
Crystal Springs South
FIGURE 15

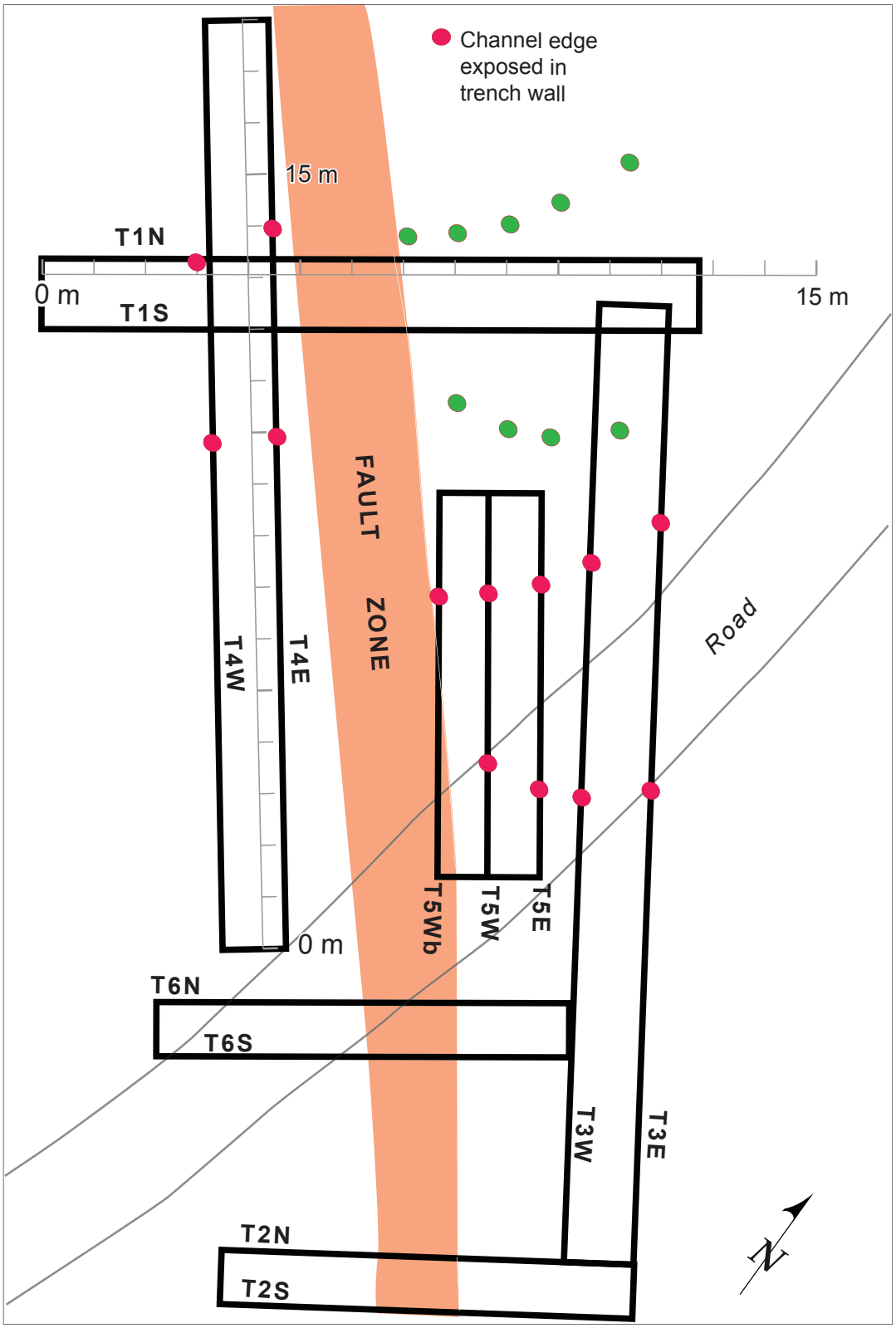

Pink dots show the locations of the channel edge. Channel edges show that the offset is between about 6 and meters. Green dots show restoration of 7 meters of slip.

MAP SHOWING ALL TRENCH LOCATIONS AND OFFSET BURIED CHANNEL

Crystal Springs South

FIGURE 16

fwla-wc-file1/project/Projects/79_2000/79_223000_Crystal_Springs_South/05_Graphics